A DISSERTATION

ON

Optoelectronic and Dielectric Investigations in Ferroelectric Liquid Crystal Composites Doped With TGA Capped CdSe Quantum Dots

Submitted by

Rohit Kumar

(Roll No: 601102007)

In partial fulfillment of the requirement for the award of degree of

Master of Technology
in
Materials and Metallurgy Engineering

Under the supervision of

Dr. K.K. Raina

School of Physics and Material Science

THAPAR UNIVERSITY

PATIALA (PUNJAB) -147004

CERTIFICATE

This is to be certify that the thesis entitled **"Optoelectronic and Dielectric Investigations in Ferroelectric Liquid Crystal Composites Doped With TGA Capped CdSe Quantum Dots"** which is being submitted by **Rohit Kumar** in partial fulfillment of the requirement for the award of **Master of Technology (M.Tech.) in Materials & Metallurgical Engineering** from School of Physics and Material Science, Thapar University Patiala (India), is a record of the study conducted by him under my supervision and guidance. No part of this thesis has been submitted for the award of any other degree.

Dr. K.K. Raina 7/6/2013
Distinguished Professor and Deputy Director
School of Physics and Material Science
Thapar University, Patiala-147004 (India)

Countersigned By:

Dr. Kulvir Singh
Associate Professor and Head
School of Physics and Material Science
Thapar University, Patiala-147004 (India)

Dr. S. K. Mohapatra
Dean of Academic Affairs
Thapar University,
Patiala-147004 (India)

ACKNOWLEDGEMENT

Several people have collaborated in the development and accomplishment of my dissertation work.

I would like to express my sincere gratitude to my esteemed and worthy supervisor **Dr. K.K. Raina, Deputy Director and Distinguished Professor, School of Physics and Material Sceince,** Thapar University for his insight help, guidance, effective supervision and thought provoking discussions during the course of the present investigation. His wide knowledge, logical way of thinking and whole hearted co-operation has been of a great value for me. His visionary thoughts have influenced me greatly. His dynamical attitude has empowered me with zeal of energy to conquer the minor details of my research work.

I would also like to thank **Dr. Kulvir Singh, Professor and Head, School of Physics and Material Sceince** for his support and providing facilities in the department.

My sincere thanks to **Dr. Manoj Sharma, P.G. Incharge, School of Physics and Material Science,** Thapar University for his support and encouragement.

I am deeply indebted to **all my Teachers, School of Physics and Material Science,** Thapar University who never turned me down whenever I seek their help. Their ideas and concepts made a remarkable influence on my understanding in the field of Physics.

I am very grateful to Ph.D. research scholar **Mr. Rishi Kumar** who always being a good support and guided me throughout my project work.

I wish my heartfelt thanks to Ph.D. research scholars **Mrs. Supreet, Mrs. Ramneek Kaur, Mrs. Gurpreet Kaur, Mrs. Manju Midha, Dr. Ravi K. Shukla** and my friends **Srishti, Hitesh, Rohit and Umash** for their generous work and good wishes.

I am very grateful to **University Grant Comission (UGC) and Department of Science and Technology (DST), New Delhi** for providing grant for research project.

I have no words to express thanks to my parents for their love, blessings and for always being with me for every step of the way.

(Rohit kumar)

ABSTRACT

The quantum confined II-VI semiconductor material becomes interesting area of research due to its large photonic band gap. A series of thiol capped CdSe quantum dot has been synthesized at different temperature in aqueous solution using thioglycollic acid ($HSCH_2COOH$, TGA) as stabilizer and optimized reaction temperature 85^oC for the growth of CdSe quantum dots, heaving high quantum yield corresponding to photoluminescence. The overall growth mechanism of CdSe quantum dots depends upon the various factors affecting the experimental conditions, including the Se-to-Cd ratio, temperature, time, and precursor concentration, which was optimized with the help of different set of experiments and getting characterized for their optical properties with the help of UV-Vis and Photoluminescence spectroscopy.

Fluorescence spectroscopy revealed that the valence band of CdSe quantum dot is situated at higher energies with respect to the radox level of most thiols, and hence inhibiting hole trapping as a result of that maintains a high luminescence efficiency. The average size (7nm) of TGA capped CdSe quantum dots prepared at 85^oC was confirmed by Transmission Electron Microscopy (TEM) and getting dispersed into ferroelectric liquid crystal for improvement in electro-optic switching and molecular relaxation behaviour of CdSe quantum dot doped FLC composites with the help of polarization rewersal technique and dielectric spectroscopy. Temperature dependent dielectric properties of dielectric properties of 0, 0.25, 0.5,1 weight % CdSe doped FLC was investigated, which shows the phase transition behaviour in CdSe doped FLC composites. Polarization switching current response of these composites shows the improvement in electrical switching, which reflects the switching response time.

CONTENTS

Chapter 1: Introduction

Matter is defined as:

It is any substance which has mass and occupies space. All physical objects are composed of matter. Which exists in three states:-

a) Solid
b) Liquid
c) Gas

Each has some characteristics feature which distinguishes one from the other. During heating, ice to water is an example of these three states for a single compound. Like solid has order and liquid has disorder.

Some substances can exist in states other than solid, liquid, and vapor. For example, cholesterol myristate (a derivative of cholesterol) is a crystalline solid below 71^{o}C. When the solid is warmed to 71^{o}C, it turns into a cloudy liquid. When the cloudy liquid is heated to 86^{o}C, it becomes a clear liquid. Cholesterol myristate changes from the solid state to an intermediate state (cloudy liquid) at 71^{o}C and from the intermediate state to the liquid state at 86^{o}C. Because the intermediate state exits between the crystalline solid state and the liquid state, it has been called the liquid crystal state.

1.1. Liquid Crystal

Liquid crystals [**1-4**], as their name implies, are substances that exhibit properties of both liquids and crystals. Specifically, these molecules possess high **orientational order** as well as the **low positional order** depending on nature. Most liquid crystals are thermotropic; their degree of orientational and positional order depends on temperature and so their liquid crystalline phase occurs within a limited temperature range between the solid and liquid phase.

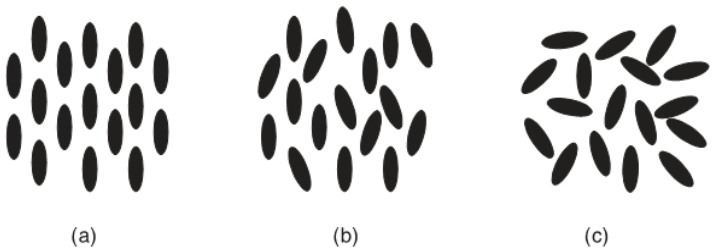

Fig 1.1: The schematics of (a) crystal, (b) liquid crystal and (c) liquid.

The term liquid crystal describes a state of matter that exhibits between the anisotropic (solid) crystal and the isotropic (liquid) liquid. The liquid crystalline or mesomorphic substances exhibits strong anisotropic in certain properties, yet certain maintain a certain extent of fluidity. Liquid crystals were first discovered in 1888, by Austrian chemist **Friedrich Reinitzer**; but the first detailed observations characterizing these phase were made by Lehmann (1890).

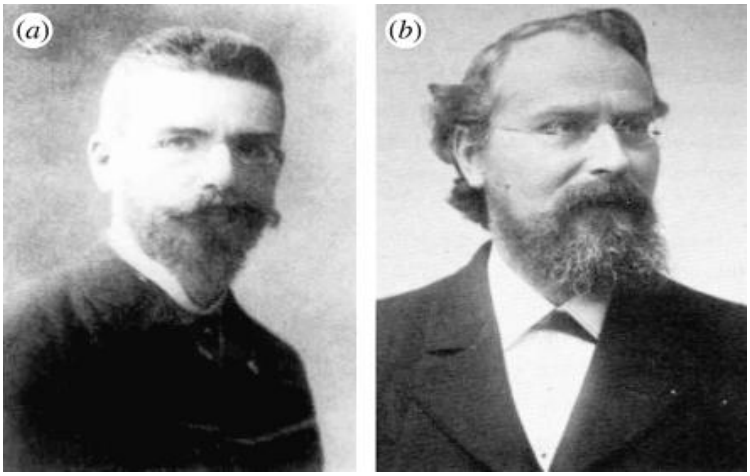

Fig 1.2: Reinitzer (Reproduced with kind permission from Merck KGaA, Germany) and (b) Lehmann (Universitätsarchiv Karlsruhe).

Liquid crystal phases, almost without exception, appear in a class of molecules called mesogens, which is derived from the Greek phrase ‘species in between’. These molecules possess an anisotropic shape, i.e. either their molecular axes have differing lengths or the properties of the constituent parts of the molecules vary (e.g. hydrophobic–hydrophilic or rigid–flexible parts). In addition, in order to display mesogenic properties, the molecules have to interact with each other through non-covalent interactions. These intermolecular

interactions are mainly responsible for the liquid crystalline properties exhibited by mesogenic materials and for their interactions with the surface (vide infra), which are critical for device applications. In order to fully appreciate how a liquid crystalline device can be modified or manipulated by these interactions, it is worthwhile to highlight the basic principles of liquid crystals, from the molecules involved through to the phases they form; all of which are a result of intermolecular forces. A liquid crystal is a substance that behaves optically like a crystal, but flows like a liquid. Overall, the molecules of a liquid crystal have the same orientation. A unit vector called the director is used to designate the preferred orientation of the molecules in a liquid crystal. By convention this vector is symbolized by the letter n. An important property of the director is that "n and –n" are equivalent vectors

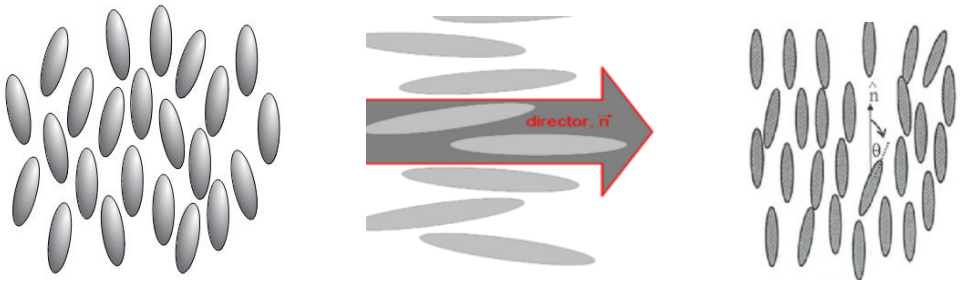

Fig 1.3: Schematic representation of molecules in thermotropic liquid crystal(nematic liquid crystal).

A highely anisotrophic shape of the molecules is necessary for mesomorphism, like for example the long and narrow rod-like or disc like shape. The transition to mesophase can take place due to purely thermel processes (thermotropic mesomorphism) or due to the influence of solvents (lyotropic mesomorphism). The fig. 1.3 shows the molecular structure of a typical rod-like liquid crystal molecule. It consists of two or more ring systems connected by a central linkage group.

Although the phenomenon of liquid crystallinity was discovered in 1888 and the term of "liquid crystals" was first used in 1890 (Priestley 1974; Meier, Sackmann et al. 1975; Hans and Rolf 1980; Finkelmann 1987; Pavel, Ball et al. 2002) liquid crystallinity has attained prominence only in the last two decades. Liquid crystals can exhibit intermediate phases where they flow like liquids but possess some physical properties of crystals. Accordingly, they are also called mesogens and various intermediate phases in which they could exist are termed mesophases or mesomorphic phases. LCs are anisotropic materials

whose flow properties strongly depend on their structures and molecular orientation. The mesomorphic phases appear as a more or less viscous fluid which can be identified visually by their characteristic turbidity or by optical birefringence. Many organic compounds, including macromolecules, would possibly form liquid crystals when they are heated above their melting temperatures. The well-known and widely studied liquid crystals are thermotropic and lyotropic (Priestley 1974; Meier, Sackmann et al. 1975; Hans and Rolf 1980). Thermoropic liquid crystals are of interest both from the standpoint of basic research and also for applications in electro-optic displays [5-7], grating [8], shutter [9-12] temperature and pressure sensors (Meier, Sackmann et al. 1975). Lyotropic liquid crystals, on the other hand, are of great interest biologically and appear to play an important role in living systems (Meier, Sackmann et al. 1975). Depending on temperature, pressure, constitutes, concentration, substitutes, and so on, mesogens can exhibit rich mesophases, including nematic (N), smectic (S), cholesteric (Ch), and blue phase (Priestley 1974; Meier, Sackmann et al. 1975; Hans and Rolf 1980; Finkelmann 1987; Leadbetter 1987).

1.1.1 Characterizing Liquid Crystals

The following parameters describe the liquid crystalline structure:

- Orientational order: Measure of the tendency of the molecules to align along the director
  on a long-range basis.
- Positional order: The extent to which the position of an average molecule or group of molecules shows translational symmetry.
- Bond orientational order: Describes a line joining the centers of nearest-neighbor molecules without requiring a regular spacing along that line. Thus, a relatively long-range order with respect to the line of centers but only short range positional order along that line.

1.1.2 Chemical Structure of Liquid Crystals:

Most liquid crystalline molecules are highly anisotropic and to a good approximation they can be regarded as rigid rods or ellipsoids of revolution with lengths is greater than their widths. The basic structure of low molecular mass liquid crystals or monomers of liquid crystalline polymers is schematically shown below

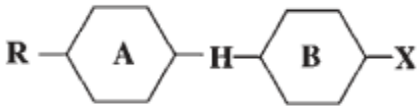

where X is a side group, R is a terminal group, A and B are aromatic rings, and H is a linking group.

1. Side group:

The following side chains are extensively studied: alkyl group (C_nH_{2n+1}); alkoxy group ($C_nH_{2n+1}O$) and alkenyl (C_nH_{2n-1}) or alkenyloxy ($C_nH_{2n-1}O$) group. The length and flexibilty of the side chain affect the type of liquid crystal phases and the phase transition. In general, for homologues, the compounds with small n show no mesogenic phase. As n increases, the monotropic liquid crystal phase appears. As n further increases the nematic phase occurs and thereafter smectic phases may appear. As n varies the even-odd alternation occurs: the compounds in odd carbon numbers in the side chains have the higher transition temperature whereas compounds in even numbers have lower transition temperatures.

2. Terminal group:

The terminal group primarily contributes to the dielectric anisotropy and the refractive indices, which in turn affects the threshold voltage and optical properties in display applications, respectively. Common terminal groups are alkyl, alkoxy, cyano, nitro, isocyanate (NCS), sulfide and halides such as F, Cl, CF_3 and OCF_3

3. Aromatic rings:

Most liquid crystal compounds consist of two or more aromatic rings. Those aromatic rings can be a totally saturated cyclo-hexane, a cyclo-cyclohexane, an unsaturated biphenyl, terphenyl, or combinations of them. Usually, the longer the ring, the higher the melting temperature.

4. Linking group:

The linking group makes an important contribution to the phase transition and physical properties such as the birefringence. The following linking groups have been well studied

- Saturated groups, such as ethylene (C_2H_4)
- Esters
- Unsaturated groups containing a double bond or a triple bond such as stilbene, azoy, schiff base, tolane or acetylene, and diacetylene.

5. Lateral group:

By substituting the hydrogen in the 2-, 3-, or 4-position of a phenyl ring by cyano, fluoro, or chloro polar group, one can modify the physical properties of liquid crystals. In most cases, the lateral substitution will broaden the molecule, thus reducing lateral attractions and lowering the nematic and smectic phase stability. Not only do the nature and size of the substitution affect the liquid crystal properties, but also the position of the group can have a significant effect.

6. Chiral center:

Replace the terminal group by a chiral center and the chiral nematic and smectic phases can be obtained. The liquid crystal molecules or monomers are generally 2–4 nm in length and 0.4–0.6 nm in width. Experiments and theories demonstrate that for compounds showing the liquid crystal phase, their axial ratio or ratio of length to width (or to diameter) must be greater than a certain value, approximately 4.

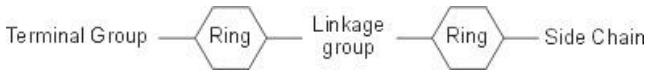

Fig 1.4: Shape of a liquid crystal molecule

1.2 Classification of Liquid Crystal

The liquid crystals **[13]** are of two types:-

- Thermotropic liquid crystals
- Lyotropic liquid crystals

A liquid crystal is a substance that behaves optically like a crystal, but flows like a liquid. Overall, the molecules of a liquid crystal have the same orientation. A unit vector called the director is used to designate the preferred orientation of the molecules in a liquid crystal. By convention this vector is symbolized by the letter n. An important property of the director is that "**n** and **–n**" are equivalent vectors.

A highely anisotrophic shape of the molecules is necessary for mesomorphism, like for example the long and narrow rod-like or disc like shape. The transition to mesophase can take place due to purely thermel processes(thermotropic mesomorphism) or due to the influence of solvents (lyotropic mesomorphism)

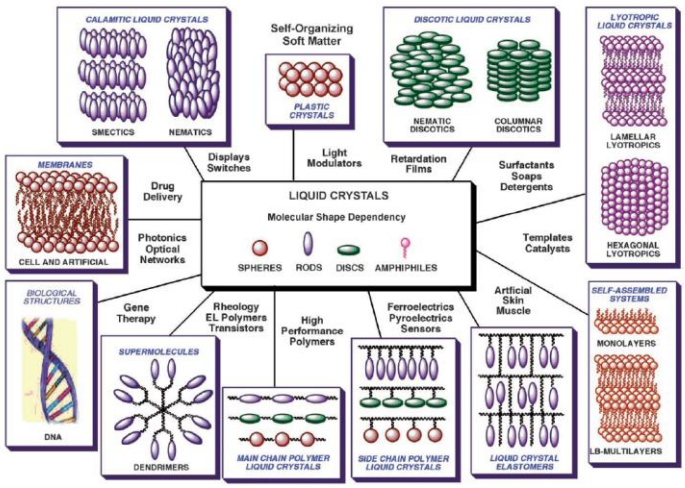

Fig 1.5: Classification of liquid crystal

1.2.1 Thermotropic Liquid Crystals

A mesogen is thermotropic [14-18] if the order of its components is determined or changed by temperature (Priestley 1974; Hans and Rolf 1980; Pavel, Ball et al. 2002). If temperature is too high, the rise in energy and therefore in motion of the components will induce a phase change. The LC will become an isotropic liquid. If, on the contrary, temperature is too low to support a thermotropic LC phase, the LC will become a crystal. The liquid crystallinity of thermotropic LC appears only in a particular temperature range, as schematically shown in Fig. 1.5. Smectic, nematic and cholesteric are three main types of thermotropic LC phases (Pavel, Ball et al. 2002).

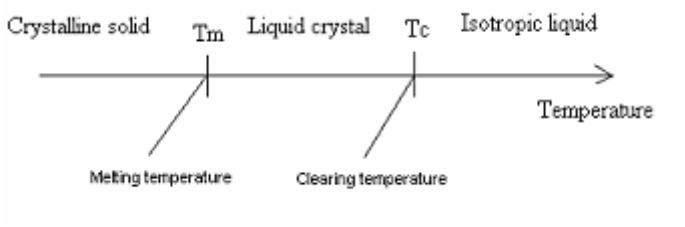

Fig 1.6: Thermotropic liquid crystalline transition. (Pavel, Ball et al. 2002)

There are a number of sub-classifications in smectic liquid crystals in terms of position and direction arrangements of molecules. In addition, the complicated textures of thermotropic LCs have been designated by the observations of columnar and blue phases.

I.2.1 (a): Nematic Liquid Crystals

Nematic liquid crystals [19-23] differ from ordinary liquids by a long range orientational order of the long molecular axes and the long molecular axes are aligned parallel to a preferred direction (Cladis and Kleman 1972; Cladis 1974; Priestley 1974), as seen in Fig.1.7. The molecules are allowed to rotate freely about their long axes and the axes of symmetry are identical with the preferred axis of the structure. Although the molecules are directionally correlated, they are positionally random or the centers of gravity are randomly distributed like an ordinary liquid. The physical properties of nematic molecules are the same along the direction of alignment and optically uniaxial direction. Characteristic "Schlieren" texture is observed in nematic director (Fig.1.8 (a) and (b)) the dark threads that are observed throughout the colored regions correspond to molecular domains which are aligned with one of the optical polarizer.

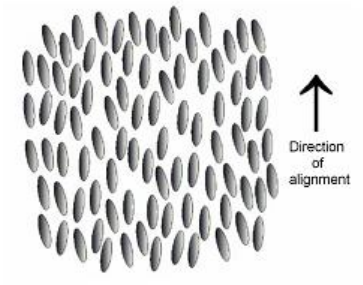

Fig 1.7: Schematic representation of molecular arrangements in nematic.

1.2.1(b): Smectic Liquid Crystals

Smectic liquid crystals [24-28] have a layered structure as presented in Fig 1.8 (b). The position of smectic molecules is correlated in some ordered patterns. Unlike nematic liquid crystals, X-ray diffraction from smectic phase would exhibit diffraction peaks due to the position order. The centers of gravity of the elongated molecules are arranged in equidistant planes (Cladis 1974; Cladis 1976; Fayolle, Noel et al. 1979). The long axes of smectic molecules are parallel to a preferred direction that may be normal to the planes (smectic A) or tilted by a certain angle (smectic C). The arrangement of the centers of gravity within the plans may be at random or regular. Typical textures of smectic liquid crystals, such as fan-shaped, focal conic, and Schlieren textures, are presented in Fig.1.10.

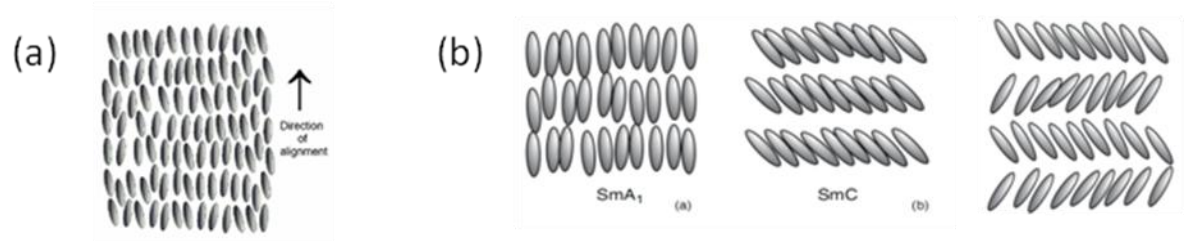

Fig. 1.8: a). Schematic representation of molecular arrangements in smectic.

b). Schematic representation of the smectic A, smectic C and smectic O phases

1.2.1(c): Cholesteric Liquid Crystals

Cholesteric phase [29-32] is often referred to as "twisted nematic" or "chiral nematic" phase but differs significantly in that the director (the unit vector describing the average direction of molecular long axes) is not constant in space (Candau, Le Roy et al. 1973; Saupe 1973; Bonnett, Jones et al. 1989). The cholesteric phase is characterized by layers of nematic molecules where each layer is twisted with respect to the ones above and below it. As a succession of layers is passed through, the director turns through 360 (as shown in Fig.1.9) and the thickness of such a period represents a pitch length of the helix. The fingerprint texture of cholesteric phase is shown in Fig.1.10. The cholesteric fingerprint texture is observed for samples with a helical pitch in the order of several micrometers. The helix axis basically lies in the plane of the substrate, i.e. in the plane of the image and the distance between adjacent dark lines is equal to the half the pitch of a helical superstructure. The main chemical feature which distinguishes a cholesteric material from an nematic liquid crystal is that its molecular structure is chiral and therefore not super imposable on its mirror image.

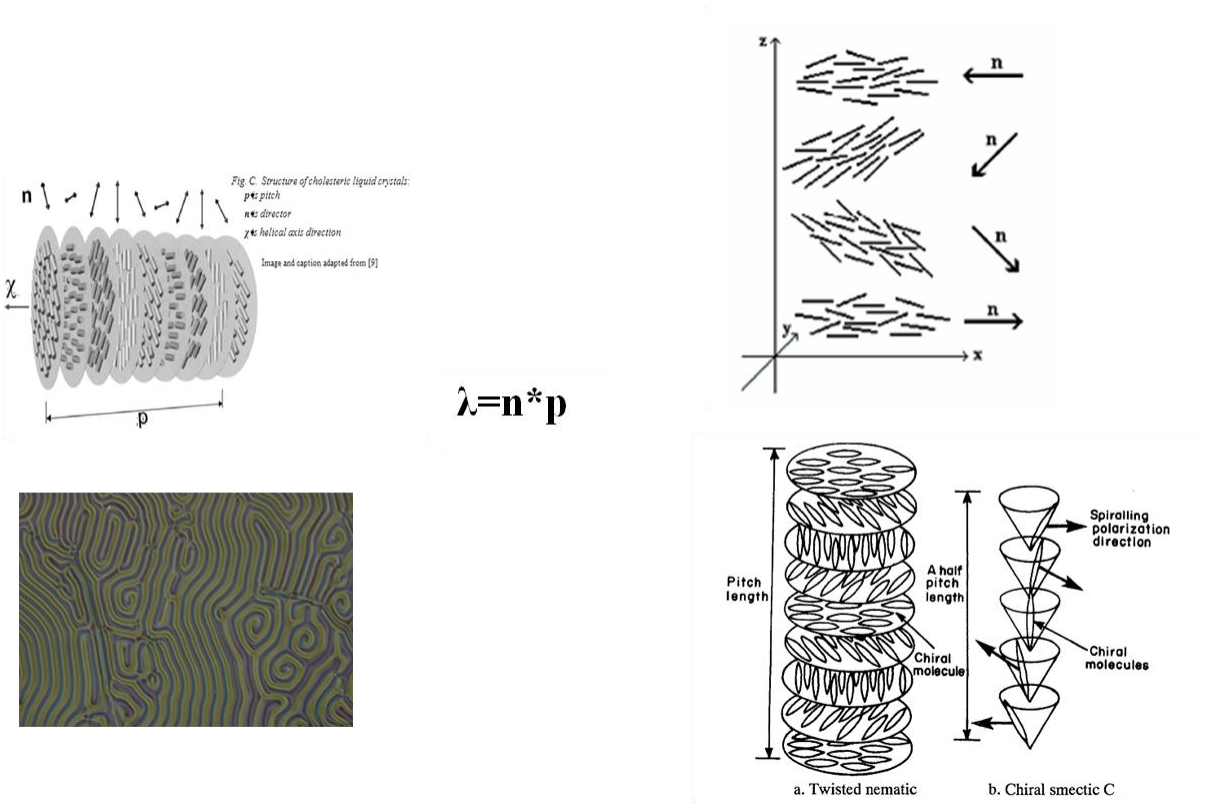

Fig. 1.9 Schematic representation of cholesteric liquid crystalline phase.

The importance of structural optical activity and the special relationship between the N and Ch phases have been demonstrated by two noteworthy observations (Levine 1974; Priestley 1974).

- ❖ N phases are made Ch by dissolving in their optically active enantiomers which themselves may or may not be LC materials.
- ❖ A racemate exhibiting an N phase can be resolved into its enantiomers, each of which will exhibit a Ch phase. A further point to note is that the helical twist senses of the phases formed by the two enantiomers are opposite in sign, indicating a relationship of helical sense to molecular structure.

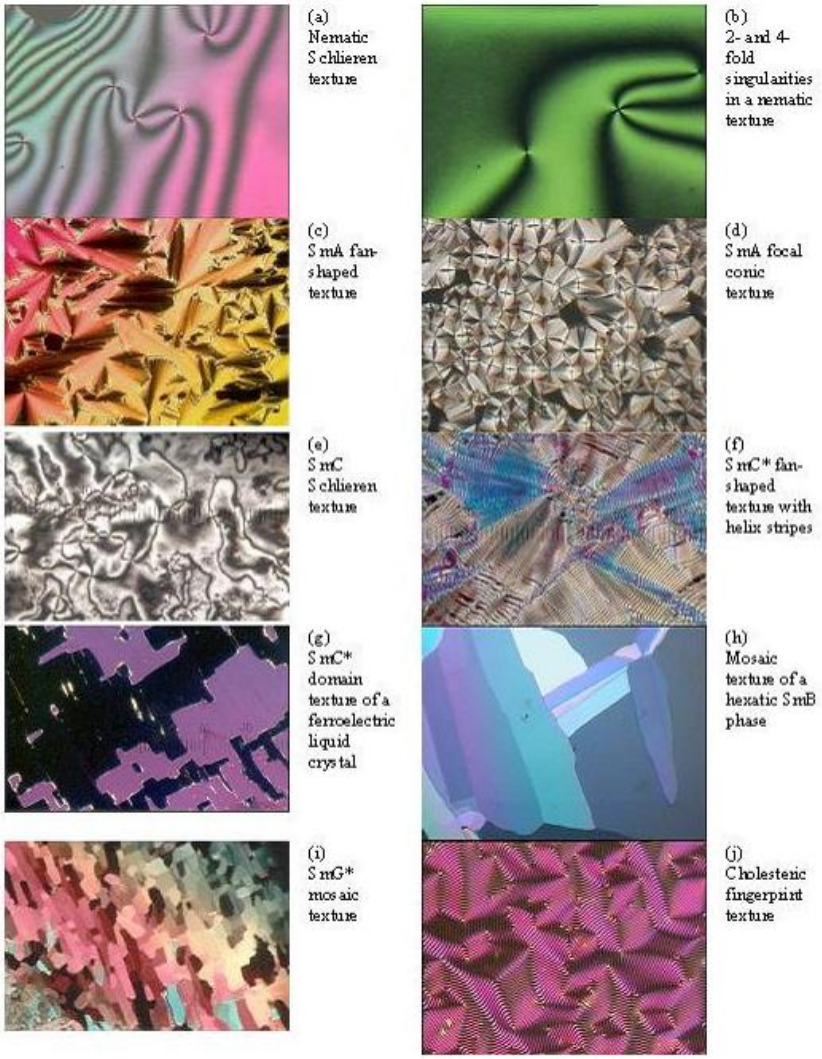

Fig 1.10: Some textures of the basic types of LCs. (Drzaic 1995)

1.2.2: Lyotropic Liquid Crystals

There is a class of materials that exhibit liquid crystal behaviour only when in solution with a solvent. Liquid crystalline phases formed in such solutions are said to be lyotropic (Priestley 1974; Hans and Rolf 1980). A lyotropic LC [36-40] can consist of two or more components that exhibit liquid-crystalline properties in appropriate concentrations. Lyotropic liquid crystalline transition process is presented in Fig.1.11. In lyotropic phases, solvent molecules fill the space around the compounds to provide fluidity to the system. In contrast to thermotropic LCs, the lyotropics have another degree of freedom of concentration that enables them to induce a variety of different phases.

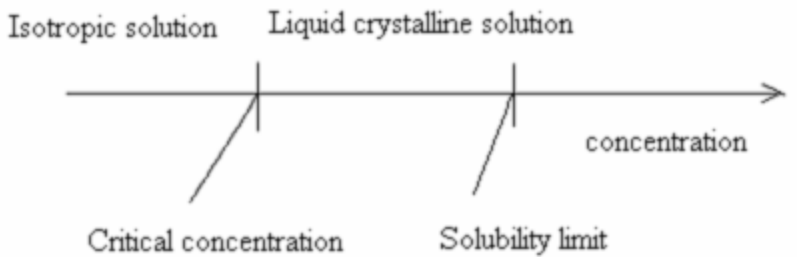

Fig 1.11: Lyotropic liquid crystalline transition. (Pavel, Ball et al. 2002)

A molecule which possesses immiscible hydrophilic and hydrophobic parts is called an amphiphilic molecule (Priestley 1974; Hans and Rolf 1980). Many amphiphilic molecules show lyotropic liquid-crystalline phase sequences depending on the volume balances between the hydrophilic part and hydrophobic part. These structures are formed through the micro-phase segregation of two incompatible components on a nanometre scale. Soap is an everyday example of a lyotropic LC (Finkelmann 1987; Drzaic 1995). The content of water or other solvent molecules changes the self-assembled structures of amphiphilic molecules. At very low concentrations, amphiphilic molecules will be dispersed randomly without any ordering. At slightly higher (but still low) concentrations, amphiphilic molecules will spontaneously assemble into micelles or vesicles. This is done so as to 'hide' the hydrophobic tail of the amphiphile inside the micelle core, exposing a hydrophilic (water-soluble) surface to aqueous solution. These spherical objects do not order. A typical phase is a hexagonal columnar phase, where the amphiphiles form long cylinders that arrange themselves into a roughly hexagonal lattice or the middle soap phase.

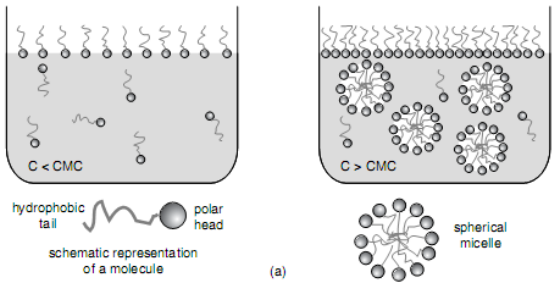

Fig 1.12: Micelle formation in Lytrophic crystal

As the concentration is further increased, a lamellar phase may form, wherein extended sheets of amphiphiles are separated by thin layers of water. For some systems, a cubic (also called viscous isotropic) phase may exist between the hexagonal and lamellar phases, wherein spheres are formed that create a dense cubic lattice. These spheres may also be connected to one another, forming a bicontinuous cubic phase. The objects created by amphiphiles are usually spherical (as in the case of micelles), but may also be disc-like (bicelles), rod-like, or biaxial (all three micelle axes are distinct) (Yang, Kikuchi et al. 2003). These anisotropic self-assembled nano-structures can then order themselves in much the same way as LCs do, forming large-scale versions of all the thermotropic phases (such as a nematic phase of rod-shaped micelles).

For some systems, at high concentration, inverse phases are observed. That is, one may generate an inverse hexagonal columnar phase (columns of water encapsulated by amphiphiles) or an inverse micellar phase (a bulk LC sample with spherical water cavities). A generic progression of phases, going from low to high amphiphile concentration, is (Kronberg, Bassignana et al. 1978; Hans and Rolf 1980; Finkelmann 1987):

- Discontinuous cubic phase (micellar phase)
- Hexagonal columnar phase (middle phase)
- Bicontinuous cubic phase
- Lamellar phase
- Bicontinuous cubic phase
- Reverse hexagonal columnar phase
- Inverse cubic phase (Inverse micellar phase)

Even within the same phases, their self-assembled structures are tunable by the concentration: for example, in lamellar phases, the layer distances increase with the solvent volume. Since lyotropic LCs rely on a subtle balance of intermolecular interations, it is more difficult to analyse their structures and properties than those of thermotropic LCs.

1.3 Quantum Dot:

Quantum dots (QDs) are semi-conducting nano crystalline structures, ranging from 2 to 100 nm depending on the types of surface coating or functional group added (Lewinski et al.

2008), made from materials such as cadmium selenide or cadmium telluride (Tan and Zhang 2005). For biological applications, QDs typically have a core/shell conjugate structure, with the core composed of atoms from groups II–VI (e.g. CdSe, CdTe, CdS, PbSe, ZnS, and ZnSe) and groups III–V (e.g. GaAs, GaN, InP, and InAs) on the periodic table (Lewinski et al. 2008). QDs absorb white light which is then re-emitted as a specific colour after a couple of nanoseconds. QDs range from 10 to 250 atoms in diameter and contain anywhere from 100 to 20000 electrons. Energy levels of QDs can be controlled by changing their shape and size in order to control the depth of the potential. The science of QDs started to develop during the 1980s when their potential was realised to build nano-scale computer applications in which light is used to process information. Since this time more recent medical applications have included 'molecular tagging' in order that proteins, viruses, antibodies or DNA can be tracked in the human body. In these applications, QDs behave as a 'fluorophore' absorbing energy at a particular wavelength and re-emitting energy at a different longer wavelength.

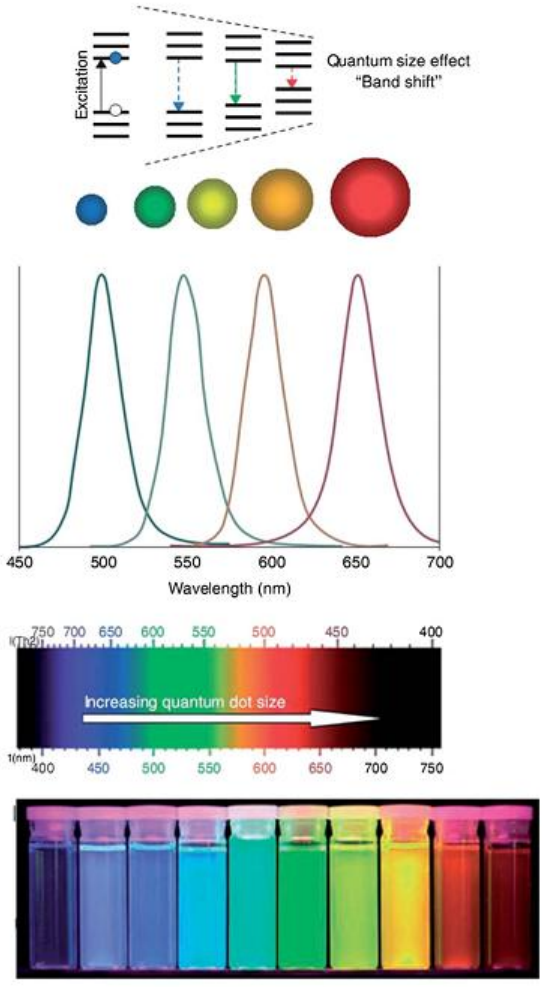

Fig. 1.13: Size-dependent PL with tuning of colors of semiconductor QDs.

Important parameters which should be taken into consideration while doping nanomaterial into liquid crystal composites are:[41]

1). Size of nanomaterial

2). Method and time of preparation of nanomaterial.

3). Solvent used for dispersion of nanomaterial in liquid crystal for example NMP,THF, DEE etc.

4). Method used for mixing whether it is centrifugation, ultrasonication or simple stirring.

5). Time

6). Nature of liquid crystal used.

7). Among all type and nature of nanomaterial (ie shape).

8). Type of alignment (whether random homogenous, or heterogeneous).

Problems in deal with nano-materials as a dopant in LC are: [42]

1). Proper dispersion of nanomaterial in LC composites cannot possible.

2). Amount of nanomaterial which is being used as a dopant is very less (usually.01wt % upto 1-2 wt% at max.) larger amount leads serious problem like agglomeration and retardation of electro optic application.

Solutions in order to overcome these problems are: [43]

1). 100% dispersion can't be achieved even with mechanical method like sonification. But sufficient mixing can be achieved by performing sonification for longer time (even though this can damage the basic properties of solvent).

2). Proper dispersion can also by using proper capping agent.

3). We used to functionalized the given nanomaterials

1.4. Review of Literature:

Various research group from the globes have made an attempts to improve the optical and dielectric properties of FLC by dispersing nanomaterials. The improved properties are listed below in literature

- In 2007, **X. Tong** et al. [44] have investigated the liquid crystal gel dispersed quantum dots system and obtained the self assembled physical network.
- In 2008, **H. Qi** et al. [45] studied the effect of functionalized nanomaterials on the optical (texture, alignment, defect formation, luminescence) and electro-optic properties of nematic liquid crystal composites.

- In 2009, **R. Basu** et al. [46] investigated process of self-assembly of quantum dots in a nematic liquid crystal.
- In 2009, **B. Kinkead** et al. [47] investigated the effect of size, capping agent and concentration of quantum dot (CdSe and CdTe) on the optical and electro-optic properties of the liquid crystal.
- In 2010, **A. Kumar** et al. [48] studied that doping of cadmium telluride quantum dots CdTe-QDs in different ferroelectric liquid crystals FLCs (LAHS19, LAHS18, FLC 6304, and KCFLC 7S) and observed pronounced memory effect.
- In 2010, **N. A. Shurpo** et al. [49] studied the effect of CdSe/ZnS semiconductor quantum dots on the dynamic properties of nematic Liquid- Crystal composite and observed that the presence of QDs leads to reduction in the time of transformation of liquid crystal molecule from planar to homeotropic position.
- In 2011, **A. Anczykowska** et al. [50] investigated that on the doping of metallic and semiconductor quantum dot leads to an strong enhancement of optical properties of hybrid liquid crystal composite.
- In 2011, **A. Kumar** et al. [51] studied that addition of quantum dot (CdTe) in different liquid crystal (LAHS18, CS1016, KCFLC7S, FELIX 17/100, SCE-13, CS1026) composites leads to an alteration in the alignment and dielectric anisotropy.
- In 2011, **E. A. Konshina** et al. [52] investigated the effect of doping of different sized and different concentration [0.1–0.2 wt %] of CdSe/ZnS quantum dots on the optical and Electrical properties of positive dielectric anisotropic nematic liquid crystal (cyanobiphenyls).
- In 2011, **A. Kumar** et al. [53] studied the effect of doping of cadmium telluride quantum dots (CdTe QDs) on the electro-optical properties of ferroelectric liquid crystals (LAHS19). [50]
- In 2011, **Javad Mirzaei** et al. [54] studied the effect of doping of magic-sized nanocrystals (MSNCs) semiconductor CdSe quantum dot on the optical, alignment and electro-optic properties of a nematic liquid crystal.
- In 2012, **A. Kumar** et al. [53] studied that study that on the dispersion of TOP/TOPO capped CdSe quantum dot leads to the enhancement of diffraction efficiency in nematic LC cells.

- In 2012, **A. L. Rodarte** et.al [54] study the ability to control and direct self-assembly of nanostructures into specific geometries with new functionalities, while preserving their original optical and electronic properties.
- In 2012, **S. G. Lukishova** et al. [55] demonstrates the coupling between quantum dot fluorescence and the cholesteric microcavity.
- In 2012, **A. Kumar** et al. [56] studied the effect of doping of ZnS quantum dot on the photoluminescence property of ferroelectric liquid crystal (KCFLC 7S).
- In 2013, **S. K. Gupta** et al. [57] studied the effect of doping of CdSe quantum dot on the electro-optic properties of FLC (DOBAMBC) in Sm A* phase.
- In 2013, **A. Kumar** et al [58] studied the effect of dispersion of doping of ZnS and CdS quantum dots in FLC mixtures (LAHS 19 and KCFLC 7 S). and they concluded that addition of quantum dots leads to enhancement in PL intensity and significantly shift the emission emission band of FLC mixture.

References

1. P. S. Drzaic (1995). Introduction. Liquid Crystal Dispersions. H. L. Ong. Singapore, World scientific publishing Co. Pte. Ltd. 1: 1-9.
2. Y. C. Su, C. C. Chu, W. T. Chang & V. K. S. Hsiao, "Characterization of optically switchable holographic polymer-dispersed liquid crystal transmission gratings", Optical Material **34** (2011) 251–255.
3. W. Huang , S. Deng , W. Li , Z. Peng, Y. Liu , L. Hu & L. Xuan, "A polarization-independent and low scattering transmission grating for a distributed feedback cavity based on holographic polymer dispersed liquid crystal" , Journal of Optics, **13** (2011) 085501.
4. R. Chan, y. King & F. Roussel, "Transparent carbon nanotube-based driving electrodes for liquid crystal dispersion display devices", Applied Physics A, **86** (2007) 159–163.
5. D. Cupelli, F. P. Nicoletta, S. Manfredi, M. Vivacqua, P. Formoso, G. D. Filpo & G. Chidichimo, "Self-adjusting smart windows based on polymer-dispersed liquid crystals" Solar Energy Materials & Solar Cells, **93** (2009) 2008–2012.
6. M. Tang, A.S Redler, D. Topgaard, C. Schmidt & H. S. Kitzerow, "Kinetics of the grating formation in holographic polymer-dispersed liquid crystals: NMR measurement of diffusion coefficients", Colloid & Polymer Science, **290** (2012) 751–755.
7. Z. Zheng, L. Zhou, D. Shen & L. Xuan, "Holographic polymer-dispersed liquid crystal grating with low scattering losses", Liquid Crystals, **39** (2012) 387–391.
8. R. Kumar & K.K.Raina, "Polymer stabilized liquid crystals: materials, physics and applications", AIP Conf. Proc., **46** (2011) 1393.
9. J.L. Fergason, "Encapsulated liquid crystal and method". U.S patent. 4, 435, 047, 1984.
10. N-H. Park, S-II Park & K-Do Suh, "A novel method for encapsulation of a liquid crystal in mono-disperse micron sized polymer particles", Colloid & Polymer Science, **279** (2001) 1082-1089.
11. L.J.Taylor, "Preparation of liquid crystal containing polymeric structure" US patent. 4, 101, 207, 1978.

12. Y. J. Liu, X. Ding, S.C. S. Lin, J. Shi, I. K. Chiang, & T. J. Huang, "Surface Acoustic Wave Driven Light Shutters Using Polymer-Dispersed Liquid Crystals" Advanced Material **23** (2011) 1656–1659.
13. P. S. Drzaic,"Liquid Crystal Dispersion" World Scientific Singapore, 1995.
14. J. W. Doane, N. A. Vaz, B. G. Wu & S. Zumer, "Field Controlled light scattering from nematic micro-droplets" Applied. Physics Letter **48 (**1986) 269-71.
15. J.W. Doane, G.Chidichimo & N.A.Vaz, "Light modulating material comprising a liquid crystal dispersion in a plastic matrix". US patent. 4,688, 900, 1987.
16. T. L. Leon & A. F. Nieves, "Drop and shells of liquid crystal" Colloid & Polymer Science, **289** (2011) 345-359.
17. O. V. Yaroshchuk, L. O. Dolgov & A. D. Kiselev, "Electro-optics and structural peculiarities of liquid crystal nano-particle-polymer composites" Physical Review E **72** (2005) 051715-1.
18. Alfonso Hinojosa and Suresh C. Sharma, "Effects of gold nano-particles on electro-optical properties of a polymer-dispersed liquid crystal", Applied Physics Letters **97** (2010) 081114 -1.
19. O.V. Yaroshchuk & L.O. Dolgov, "Electro-optics and structure of polymer dispersed liquid crystals doped with nano-particles of inorganic materials" Optical Materials **29** (2007) 1097–1102.
20. R. V. Tal'roze, G. A. Shandryuk, A. S. Merekalov, A. M. Shatalova, & O. A. Otmakhova, "Alignment of Nano-particles in Polymer Matrices" Polymer Science Series A **51**(2009) 1194–1203.
21. K. Sim , S. J. Sung, E. A. Jung, D. H. Son, D. H. Kim, J. K. Kang & K. Y. Cho, "Lattice-patterned LC-polymer composites containing various nanoparticles as additives" Nanoscale Research Letters **7:46 (**2012) 2-8.
22. K. J. Yang & D. Y. Yoon, "Electro-optical characteristics of dye-doped polymer dispersed liquid crystals", Journal of Industrial and Engineering Chemistry, **17** (2011) 543–548.
23. P. Kumar & K.K. Raina, "Morphological and electro-optical responses of dichroic polymer dispersed liquid crystal films", Current Applied Physics, **7** (2007) 636–642.
24. I.I. Smalyukh, R. Pratibha, N.V. Madhusudana and O.D. Lavrentovich, "Selective imaging of 3D director fields and study of defects in biaxial smectic A liquid crystals", The European Physical Journal E, **16** (2005) 179–191.
25. H. L. Liang, S. Schymura, P. Rudquist, & J. Lagerwall, "Nematic-Smectic Transition under Confinement in Liquid Crystalline Colloidal Shells" Physical Review Letters, **106** (2011) 247801
26. J, Prakash, A. Kumar, T. Joshi, D. S. Metha, A. M. Biradar& W. Haase, "Spontaneous polarization in smectic a phase of carbon nanotubes doped deformed helix ferroelectric liquid crystal" Molecular Crystal Liquid Crystal, **541** (2011) 404]–176.
27. P. K. Mandal, A. Lapanik, R. Wipf, B. Stuehn, & W. Haase "Sub-hertz relaxation process in chiral smectic mixtures doped with silver nanoparticles", Applied Physics Letter, **100** (2012) 073112.
28. R. Manohar, A. K. Srivastava & A. K. Misra "Electro-Optical Behavior for Dye-Doped FLC",Soft Materials, **8** (2010) 1–13.
29. R. Basu, K. A. Boccuzzi, S. Ferjani, & C. Rosenblatt "Carbon nanotube-induced chirality in an achiral liquid crystal", Applied Physics Letters **97** (2010) 121908.
30. Z. Xu & C. Gao, "Graphene chiral liquid crystals and macroscopic assembled fibres", Nature Communications, (2011) 1-9 accepted.
31. B K Sadashiva " Molecular structure and chiral liquid crystalline phases", Pramana Journal of Physics, **53** (1999) 213-222.
32. S. Chandrasekhar, "Chirality in Liquid Crystals", Springer, New York, (2001) 115-120.

33. D. K. Yoon, G. P. Smitha, E. Tsaia, M. Moranc, D. M. Walbac, T. Bellinid, I. I. Smalyukha & N. A. Clark "Alignment of the columnar liquid crystal phase of nano-DNA by confinement in channels", Liquid Crystals, **39** (2012) 571–577.
34. C. V. Cerclier, M. Ndao, R. Busselez, R. Lefort, E. Grelet, P. Huber, A. V. Kityk, L. Noirez, A. Schönhals, & D. Morineau,"Structure and Phase Behavior of a Discotic Columnar Liquid Crystal Confined in Nano channels"Journal Of Physical Chemistry, **116** (2012) 18990−18998.
35. Y. Chen, D. Xu, S. T. Wu, S. Yamamoto & Y. Haseba "A low voltage and submillisecond-response polymer-stabilized blue phase liquid crystal" Applied Physics Letters **102** (2013) 141116.
36. Z. Chen, T. L. Greaves, R. A. Caruso & C. J. Drummond,"Long-range ordered lyotropic liquid crystals in intermediate-range ordered protic ionic liquid used as templates for hierarchically porous silica", **22** (2012) 10069–10076.
37. P. LIU, Q. Liang, C. Liu, X. Jian, D. Hong & Y. LI "Preparation and Characterization of Lyotropic Liquid Crystalline Aromatic Copolyamides Containing Twisty and Non-coplanar Moiety" Polymer Journal, **38** (2006) 477–483.
38. M. Nishizawa, K. Saito, & M. Sorai "Thermodynamic Study of Phase Transitions in Lyotropic Liquid Crystals: Adiabatic Calorimetry on Nonionic Surfactant $C_{12}E_6$-Water System", Journal Of Physical Chemistry B, **105** (2001) 2987-2992.
39. T. M. Dellinger & P. V. Braun "Lyotropic Liquid Crystals as Nanoreactors for Nanoparticle Synthesis", Chemistry of Mateials. (2004) **16** 2201-2207.
40. N. J. Brooks, H. A. A. Hamid, R.Hashim , T. Heidelberg , J. M. Seddon , C. E. Conn , S. M. M. Husseini , N. I. Zahid & R. S. D. Hussen "Thermotropic and lyotropic liquid crystalline phases of Guerbet branched-chain -D-glucosides", Liquid Crystals, **38** (2011) 1725–1734.
41. N. A. Hamizi, M. R. Johan "Optical Properties of CdSe Quantum Dots via Non-TOP based Route" International Journal of Electrochemical Science, **7** (2012) 8458 – 8467.
42. A. M. Nightingale & J. C. D. Mello, "Micro-scale synthesis of quantum dots", Journal of Materials Chemistry, **20** (2010) 8454–8463.
43. V. Babentsov & F. Sizov "Defects in quantum dots of II B-VI semiconductors" Opto-Electronics Review **16** (2008) 208–225.
44. X. tong & Y Zhao, "Liquid crystal gel dispersed quantum dots: Reversible Modulation of Photoluminescence intensity using an electric field", Journal of American Chemistry Society, **129** (2007) 6372-6373.
45. Qi, B. Kinkead & T. Hegmann, "Effect of functioalized metal and semiconductor nanoparticle in nematic liquid crystal phases", Proc. SPIE, **6911 (**2008) 691106/691101–691106/691111.
46. R. Basu & G. S. Iannacchione, "Evidence for directed self-assembly of quantum dots in a nematic liquid crystal", Physical Review E, **80** (2009) 010701.
47. B. kinkead & T. Hegmann, "Effects of size, capping agent and concentration of CdSe and CdTe quantum dot doped into a nematic liquid crystal on the optical and electro-optic properties of the final colloidal liquid crystal mixtre", Journal of Materials Chemistry, **20** (2009) 448-449.
48. A. Kumar, J. Prakash, M. T. Khan, S. K. Dhawan, & A. M. Biradar, "Memory effect in cadmium telluride quantum dots doped ferroelectric liquid crystals", Applied Physics Letters, **97** (2010) 163113.
49. N. A. Shurpo, M. S. Vakshtein, & N. V. Kamanina, "Effect of CdSe/ZnS Semiconductor Quantum Dots on the Dynamic Properties of Nematic Liquid-Crystalline Medium", Technical Physics Letters, **36** (2010) 319–321.

50. A. Anczykowska S. Bartkiewicz, M. Nyk, & J. Mysliwiec, "Enhanced photorefractive effect in liquid crystal structures co-doped with semiconductor quantum dots and metallic nanoparticles", Applied Physics Letter, **99** (2011) 191109.
51. A. Kumar, P. Silotia, and A. M. Biradar, "Sign reversal of dielectric anisotropy of ferroelectric liquid crystals doped with cadmium telluride quantum dots" Applied physics letters **99** (2011) 072902.
52. E. A. Konshina, E. O. Gavrish, A. O. Orlova, and M. V. Artem'ev, "Effect of dispersed CdSe/ZnS quantum dots on optical and electrical characteristics of nematic liquid crystal Cells", Technical physics letter, **37** (2011) 1011–1014.
53. A. Kumar and A. M. Biradar, "Effect of cadmium telluride quantum dots on the dielectric and electro-optical properties of ferroelectric liquid crystals" Physical review E, **83** (2011) 041708.
54. Javad Mirzaei, Martin Urbanski, Kui Yu, Heinz-S. Kitzerow and Torsten Hegmann, "Nanocomposites of a nematic liquid crystal doped with magic-sized CdSe quantum dots", Journal of Materials Chemistry, **21** (2011) 12710.
55. A. Anczykowska, S. Bartkiewicz, M. Nyk, and J. Mysliwiec, "Study of semiconductor quantum dots influence on photorefractivity of liquid crystals", Applied physics letters, **101** (2012) 101107.
56. A. L. Rodarte, C. G. L. Ferri, C. Gray, L. S. Hirst, S. Ghosh, "Directed assembly and in situ manipulation of semiconductor quantum dots in liquid crystal matrices", Proc. of SPIE, **8279** (2012) 82790
57. S. G. Lukishova, Luke J. Bissell, Justin Winkler, and C. R. Stroud,"Resonance in quantum dot fluorescence in a photonic band-gap liquid crystal host" Optics Letters, **37** (2012) 1259-126.
58. A. Kumar, J. Prakesh, Abhay D. Deshmukh, D. Haranath, P. Silotia and A.M. Biradar, "Enhancing the photoluminescence of ferroelectric liquid crystal by doping with ZnS quantum dots", Applied physics letters, **100** (2012) 134101.
59. S. K. Gupta, D. P. Singh, P. K. Tripathi, R. Manohar, M. Varia, L. K. Sagar and S. Kumar, "CdSe quantum dot- dispersed DOBAMBC: an electro-optical study", Liquid crystals,**40** (2013) 528-533.
60. A. kumar, S Tripathi, A D Deshmukh, D Haranath, P singh and A M Biradar, "Time evolution photoluminescence studies of quantum dot doped ferroelectric liquid crystal", Journal of physics D: applied physics, **46 (2013)** 195302.

Chapter 2: Experimental Techniques

2.1. Growth and Nucleation Mechanism of TGA Capped Cdse Quantum Dot:

During the synthesis of CdSe quantum dot, we choose an appropriate solvo-chemical (co-precipitation) route for the preparation. Cadmium Chloride and Selenium [purchased from S d fine chemical limited (SDFCL)] was used to prepare the precursors and Thio-glycolic acid (TGA) [purchased from S d fine chemical limited (SDFCL)] was used as a capping agent**.** The methodology of preparation of both Cadmium and Selenium source is given in the flow chart below as shown in the fig. 1.

The overall reaction mechanism during the formation of Cadmium and Selenium source involves following steps:

$Cd^{2+} + TGA \rightarrow Cd\,(TGA)^{2+}$ ……(1)

$H_2O \rightleftharpoons H^+ + OH^-$ ……(2)

$OH^- + HSe^- \rightarrow H_2O + Se^{2-}$ ……(3)

$Cd(TGA)^{2+} + Se^{2+} \rightarrow CdSe\,(TGA)$ …… (4)

$nCdSe(TGA) \rightarrow [CdSe(TGA)]_n$ ……(5)

Equations (1) and (4) demonstrate that the slightly basic solution is good for the formation of $Cd(TGA)^{2+}$complex, while the presence of stronger base leads to the formation of $Cd(OH)_2$. Here Cd^{2+}, $Se^{2-}$and TGA instantly formed CdSe (TGA) nuclei as indicated in Equation (7):

$Cd(OH)_2 \leftrightharpoons Cd^{2+} + 2OH^-$ …… (6)

$Cd^{2+} + Se^{2-} + TGA \rightarrow CdSe(TGA)$ …… (7)

Now, Cadmium and selenium source is mixed in ratio 1:3 in round bottom three neck flask under the presence of nitrogen gas atmosphere. The reflux temperature of the reaction during synthesis is optimized by different set of experiments with varying temperature and pH conditions with constant refluxing time (10 hrs.).[1-3] Yellow color appearance in the solution indicates the formation of flouroscent TGA capped CdSe quantum dots. After that the water content is removed by the centrifuge the final solution at 12000 rpm, for 15

minutes. The impurities were removed by washing CdSe QD's with ethanol solvents. Then CdSe QD's was filtered out and dried at 45^{o}C temperature in vacuum oven.

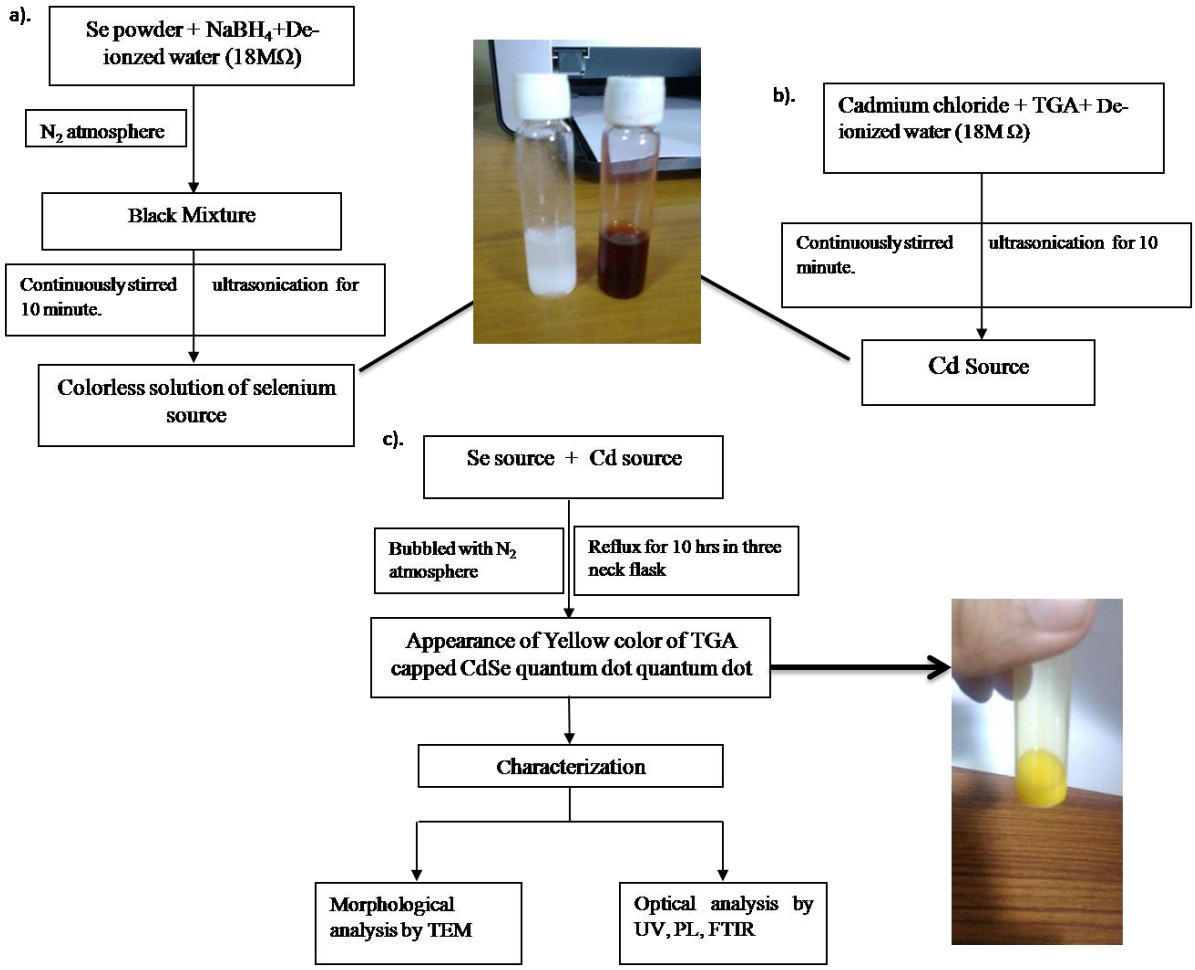

Fig 1: Flow chart for the preparation of CdSe quantum dot

In any synthesis method, Preparation of colloidal nano-crystals consists of mainly three components: 1) precursors, 2) organic surfactants and 3) solvents. And overall yield and properties of product depends on various factors like selection of preparation methods, reaction temperature, reaction time etc. Under suitable reaction conditions, the precursors chemically transform into atomic or molecular species or clusters.

A cluster can form homogeneously within the original phase or heterogeneously on various irregularities such as pre-existing small particles or ions, which assist in surmounting the free energy barrier associated with formation of an interface between the small cluster of the new phase and the original phase. The lifetime of clusters is extremely short, but since a very

large number of clusters form and dissociate at any time, a few can reach the critical size and continue to grow spontaneously to form larger particles. They undergo nucleation process and leads to the formation of final product (nano-crystals).

Formation of molecular clusters occurs through random collisions and rearrangements of atoms or molecules of the existing phase. Growth of a cluster can be represented as a reversible stepwise kinetic process. From an energetic perspective, the free energy of cluster formation (ΔG_f) increases with cluster size prior to but decreases after the critical nucleus, reaching a maximal value at the critical size, r=r*. After reaching a critical size, further growth of the cluster becomes spontaneous.

For $(r \rightarrow r^*)$

$$\frac{\partial \Delta G}{\partial r} = 0.$$

The rate at which nucleation occurs is related to the chemical makeup of the critical nucleus. The growth of nano-crystals involves mainly two steps: nucleation of an initial seeds or clusters, which is being followed by the growth process. For nucleation during the transformation of nuclei into final product, the Gibbs free energy is the main driving force.

This process is characterized by a decrease in both enthalpy and entropy of the nucleating system (i.e. $\Delta H < 0$ and $\Delta S < 0$). Although thermodynamically favorable according to the first law of thermodynamics, (i.e., exothermic) nucleation is hindered in entropy according to the second law of thermodynamics. A free energy barrier, ΔG ($\Delta G = \Delta H - T\Delta S > 0$), is often involved and needs to be surmounted before transformation to the new phase, which becomes spontaneous. The decrease in Gibbs free energy of the systems governs whether the transformation is feasible or favorable. Overall mechanism of nucleation and growth is shown in fig. 2. The nucleation process is not that simple and its rate as well as overall kinetics depends upon various factors like presence of surfactant molecules, direction of heat flows(or temperature gradients) and behavior of solvent used etc. Nucleation of Nano-crystals is analogous to that of freezing of liquids, crystallization of supersaturated solutions, and formation of vapor bubbles inside the bulk liquid.[4-6]

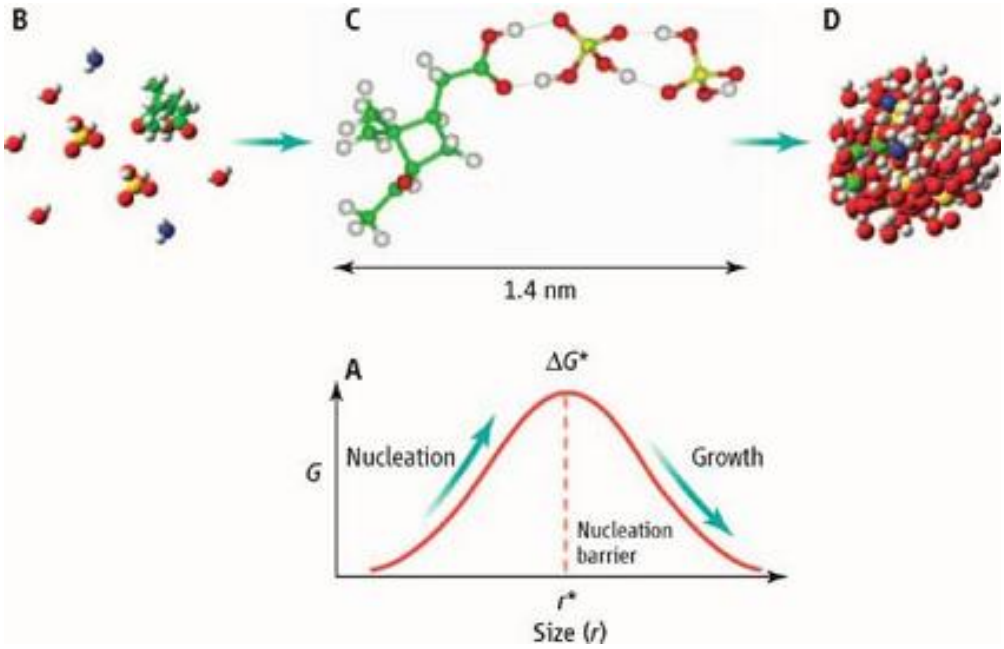

Fig 2: General outlook for the nucleation and growth phenomena

2.2 Characterization Techniques used for the Detection Of TGA Capped Cdse Quantum Dots:

Once the synthesis of TGA Capped CdSe quantum dots was done. For the characterization of formed quantum dot some instrumentation are required. These techniques are listed below:

1). FTIR (Fourier Transform Infra-Red spectroscopy)

2). UV Vis spectroscopy (Ultra-violet Visible spectroscopy)

3). PL spectroscopy (Photo-luminescence spectroscopy)

4). TEM (Transmission electron microscope)

2.2.1. FTIR (Fourier Transform Infra-Red):

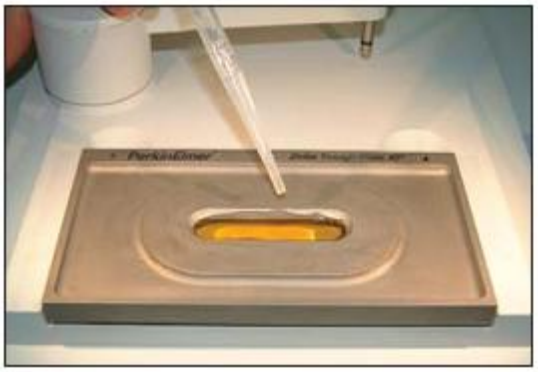

Fig 3: Sample holder for FTIR spectra

An FT-IR (Fourier Transform Infra-Red) Spectrometer is an instrument which acquires broadband NIR to FIR spectra. Infrared (IR) spectroscopy is one of the most common spectroscopic techniques used for the determination structural elucidation and compound identification**.** Simply, it is the absorption measurement of IR frequencies of different chemical bonds existing in organic sample positioned in the path of an IR beam.[6-10] The main goal of IR spectroscopic analysis is todetermine the chemical functional groups in the sample. Different functional groups absorbs characteristic frequencies of IR radiation.

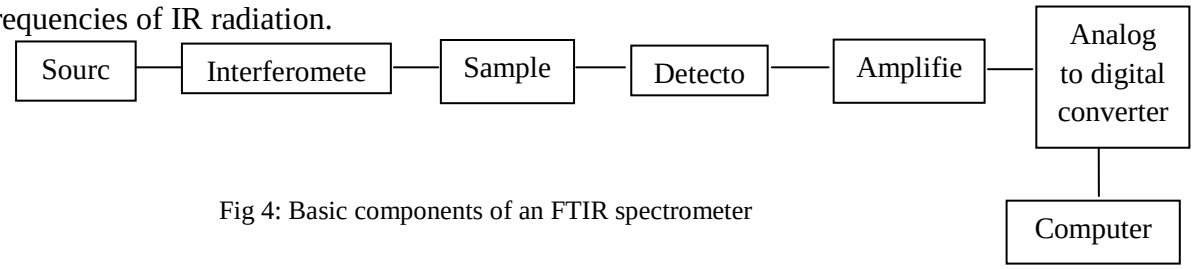

Fig 4: Basic components of an FTIR spectrometer

An FT-IR Spectrometer is a method of obtaining infrared spectra by first collecting an inter-ferogram from the sample placed on the sample holder [fig 3]. The signal using an interferometer, and then performing a Fourier Transform (FT) on the inter-ferogram to obtain the spectrum. An FT-IR Spectrometer collects and digitizes the inter-ferogram, performs the FT function, and displays the spectrum and is shown in the fig 4.

The basic phenomenon of absorption IR spectra depends upon random motion (such as rotational or vibrational) of atoms inside the molecules at room temperature. When the frequency of a specific vibration is equal to the frequency of the IR radiation

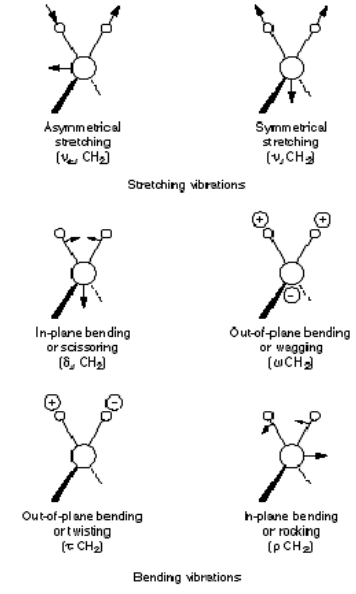

Fig 5: Different major vibrational modes for a non-linear group

directed on the molecule, the molecule absorbs the radiation, corresponding to the absorption frequency. Each atom has three degrees of freedom, corresponding to motions along any of the three Cartesian coordinate axes (x, y, z). A polyatomic molecule of n atoms has total 3n degrees of freedom. However, 3 degrees of freedom are required to describe translation, the motion of the entire molecule through space. Additionally, 3 degrees of freedom correspond to rotation of the entire molecule. Therefore the remaining 3n– 6 degrees of freedom are true, fundamental vibrations for nonlinear molecules. Linear molecules possess 3n– 5 fundamental vibrational modes because only 2 degrees of freedom are sufficient to describe rotation. Among the 3n– 6 or3n– 5 fundamental vibrations (also known as normal modes of vibration), those that produce a net change in the dipole moment may result in an IR activity and those that give polarizability changes may give rise to Raman activity. Naturally, some vibrations can be both IR- and Raman-active. The total number of observed absorption bands is generally different from the total number of fundamental vibrations. It is reduced because some modes are not IR active and a single frequency can cause more than one mode of motion to occur. Conversely, additional bands are generated by the appearance of overtones (integral multiples of the fundamental absorption frequencies), combinations of fundamental frequencies, differences of fundamental frequencies, coupling interactions of two fundamental absorption frequencies, and coupling interactions between fundamental vibrations and overtones or combination bands (Fermi resonance). The intensities of overtone, combination, and difference bands are less than those of the fundamental bands. The combination and blending of all the factors thus create a unique IR spectrum for each compound. The major types of molecular vibrations are stretching and bending. The various types of vibrations are illustrated in fig. 5. Infrared radiation is absorbed and the associated energy is converted into these types of motions. The absorption involves discrete and quantized energy levels. However, the individual vibrational motion is usually accompanied by other rotational motions. These combinations lead to the absorption bands, not the discrete lines, commonly observed in the mid IR region. For these analyses, we have used FTIR spectrophotometer (MODEL PERKIN ELMER SYSTYEM BX 51) as shown in the fig 6.

Fig 6 : FTIR system for determination of various group present in compound

2.2.2. UV Vis Spectroscopy:

Many molecules absorb ultraviolet or visible light. The absorbance of a solution increases as attenuation of the beam increases. Absorbance is directly proportional to the path length,b, and the concentration, c, of the absorbing species.

Beer Lambert law states that

$$\mathbf{A = \log_{10}\frac{I_0}{I} = e*b*c},$$

where **e** is a constant of proportionality, called the absorbtivity.

Different molecules absorb radiation of different wavelengths. An absorption spectrum will show a number of absorption bands corresponding to structural groups within the molecule. For example, the absorption that is observed in the UV region for the carbonyl group in acetone is of the same wavelength as the absorption from the carbonyl group in diethyl ketone.

2.2.2.1. Principle of UV Spectroscopy:

Absorption of visible and ultraviolet light produces changes in the electronic states of molecules associated with the electronic states of molecules associated with the excitation of an electron from a lower to a higher energy level. But it must be noted that each electronic

level in a molecule is associated with a number of vibrational sub levels (with small energy separations) and each vibrational level in turn associated with a number of rotational sub levels (with still smaller energy separation). Therefore in its transition to higher energy level, an electron can go from any of the sub levels- corresponding to various vibrational and rotational states-in the ground state to any of the sub-levels in the excited state.

2.2.2.2. The Origin of the Absorptions

Visible light lies in the wavelength range 4.0 – 7.0 x 10^{-7}m.To keep the numbers more manageable, it is usually quoted in nano-metres (10^{-9}m) so that the range becomes 400–700 nm. When light is absorbed by a material, valence (outer) electrons are promoted from their normal (ground) states to higher energy (excited) states.

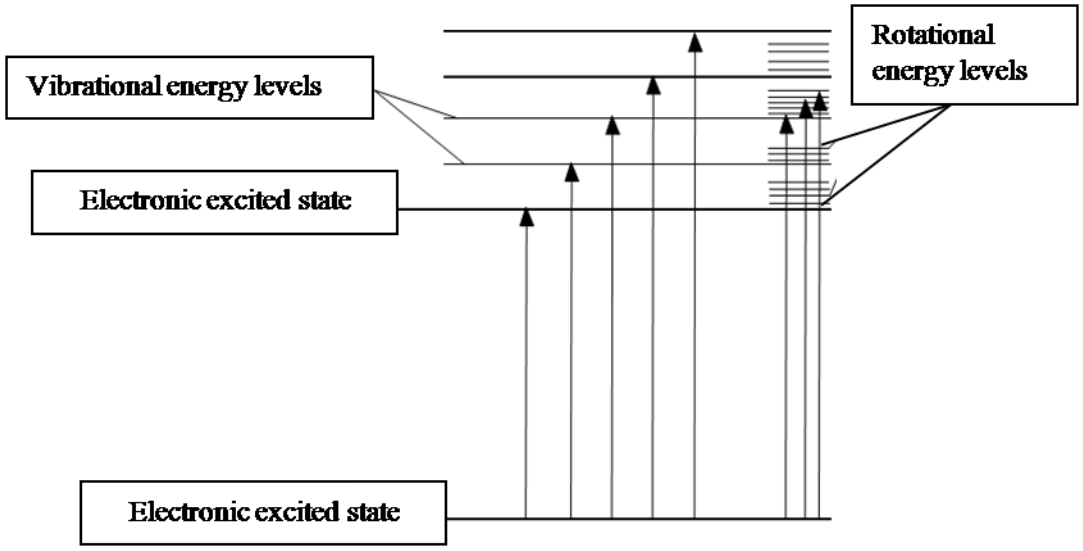

Fig 7: Electronic and vibrational levels

Valence electrons can generally be found in one of three types of electron orbital:

1). single, or σ, bonding orbitals;

2). double or triple bonds (π bonding orbitals); and

3). non-bonding orbitals (lone pair electrons).

Sigma bonding orbitals tend to be lower in energy than π-bonding orbitals [fig.7], which in turn are lower in energy than non-bonding orbitals. When electromagnetic radiation of the correct [11-14]

2.2.3. Photo-Luminescence Spectroscopy:

2.2.3.1. Luminescence

Luminescence is a science closely related to spectroscopy, which is the study of the general laws of absorption and emission of radiation by matter. The existence of luminous organisms such as bacteria in the sea and in decaying organic matter, glow worms and fireflies have mystified and thrilled man since time immemorial. A systematic scientific study of the subject of luminescence is of recent origin, from the middle of nineteenth century. In 1852 English Physicist G.C.Stokes identified this phenomenon and formulated his law of luminescence now known as Stoke's law, which states that the wavelength of the emitted light is greater than that of the exciting radiation. German physicist E. Wiedemann introduced the term 'luminescence' (weak glow) into the literature in 1888. The phenomenon in which certain kinds of substance emitting light on absorbing various energies without heat generation is called luminescence. Luminescence is obtained under variety of excitation sources. The wavelength of emitted light is characteristic of the luminescent substance and not of the incident radiation. The various luminescence phenomena are given names based on the type of radiation used to excite the emission are shown in the table 1.

Photoluminescence (PL) is the spontaneous emission of light from a material under optical excitation. The excitation energy and intensity are chosen to probe different regions and excitation concentrations in the sample. Typical experimental setup of PL instrument is outlined in the figure 8. PL investigations can be used to characterize a variety of material parameters like absorption spectrum, emission spectrum etc.

PL spectroscopy provides electrical (as opposed to mechanical) characterization, and it is a selective and extremely sensitive probe of discrete electronic states. Features of the emission spectrum can be used to identify surface, interface, and impurity levels and to gauge alloy disorder and interface roughness. PL analysis is nondestructive. Indeed, the technique requires very little sample manipulation or environmental control.

Table 1: Various luminescence phenomena and there basic details.

Type	Detail
Internal Conversion	Radiationless transition to lower state when vibrational energy levels "match
External Conversion	Radiationless transition to lower state by collisional deactivation
Intersystem Crossing	Transition with spin change (e.g. S ⟶ T)
Fluorescence	Emission not involving spin change (e.g. S⟶S, T⟶T), efficient, short-lived <10-5 s
Dissociation	Excitation to vibrational state with enough energy to break bond
Pre-dissociation:	Relaxation to state with enough energy to break bond

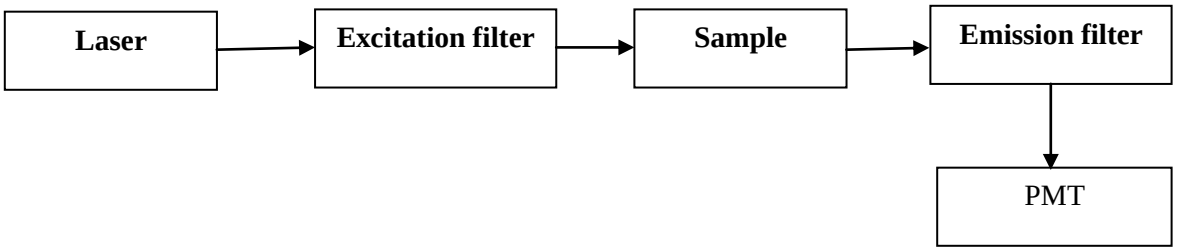

Fig 8: Typical experimental set up for PL measurements.

Because the sample is excited optically, electrical contacts and junctions are unnecessary and high-resistivity materials pose no practical difficulty. In addition, time-resolved PL can be very fast, making it useful for characterizing the most rapid processes in a material. The

fundamental limitation of PL analysis is its reliance on radiative events. Materials with poor radiative efficiency, such as low-quality indirect band gap semiconductors, are difficult to study via ordinary PL. Similarly, identification of impurity and defect states depends on their optical activity. Although PL is a very sensitive probe of radiative levels, one must rely on secondary evidence to study states that couple weakly with light.

Fig 9: Photograph of experimental set up for PL spectrophotometer [model cary eclipse in material research lab]

2.2.3.2. Factors Affecting Quantitative Accuracy

It is essential to examine the quality of solvents periodically since small traces of contaminants may be enough to produce high black values. If the solvent blank is appreciable it can usually be reduced to a reasonable value by distillation or washing with acid, base or water.

• Water is the most common solvent and de-ionized-distilled water should always be employed.

• Solvents should not be stored in plastic containers since leaching of organic additives and plasticisers will produce high blank values.

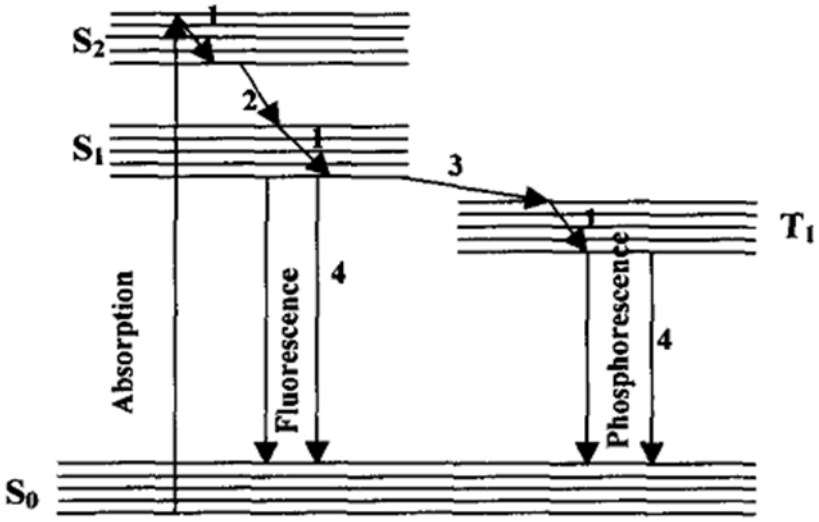

Fig 10: Partial energy level diagram of a photo-luminescent molecule. S1 & S2 are singlet states and T1 the triplet states

• All other reagents used in the assay should be carefully controlled and high quality grades are to be recommended.

• Reagent blanks should always be carried through the analytical procedure and the actual value of the blank determined before the instrument is re-zeroed.

• High or changed blank values should immediately cast suspicion upon the solvents and reagents employed.

As frequency is absorbed, a transition occurs from one of these orbitals to an empty orbital shown in fig. 10, usually an anti-bonding orbital (σ*or π*). The exact energy difference between the orbitals depends on the atoms present and the nature of the bonding system. Most of the transitions from bonding orbitals are of too high a frequency (too short a wavelength) to measure easily, so most of the absorptions observed involve only π→π*, n→σ*and n→π*transitions and are shown in the fig 11.

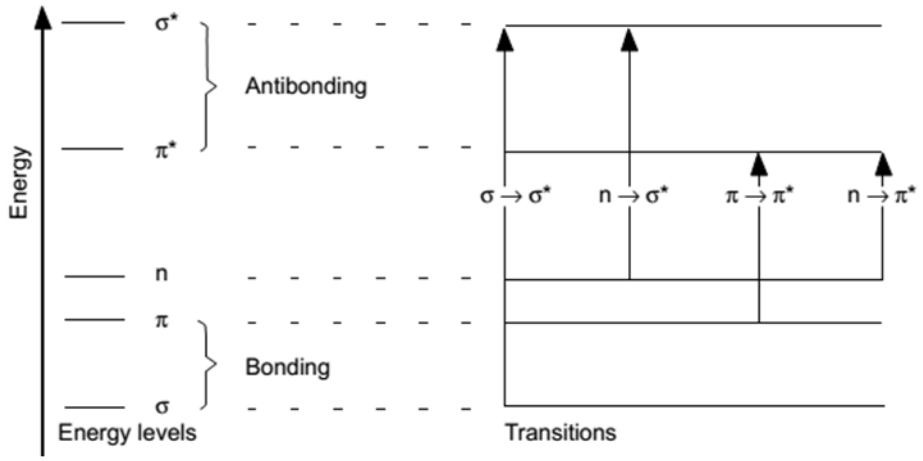

Fig 11: Electron transitions in Ultra-violet\visible spectroscopy

2.2.4. Transmission Electron Microscope:

Ernst Ruska developed the first transmission electron microscope (TEM), with the assistance of Max Knolls in 1931. After significant improvements to the quality of magnification, Ruska joined the Sieman's Company in the late 1930s as an electrical engineer, where he assisted in the manufacturing of his transmission electron microscope, which now become one of the most powerful and important characterization equipment for the quantitative as well as qualitative analysis of nanomaterials. It helps in characterizing the particle size, size distribution and morphology of nanomaterials. The basic operation of TEM is same as that of optical microscope. But here in TEM, electron replaces photons and electro-magnetic lenses replace the glass lenses. These major changes leads to significantly much higher resolution than simple light based imaging techniques. [15-17]

The basic components of transmission electron microscope (TEM) can be listed as in the fig. 12:

- An electron source
- Thermionic Gun
- Electron beam
- Electromagnetic lenses
- Vacuum chamber

- 2 Condensers
- Sample stage
- Phosphor or fluorescent screen
- Computer

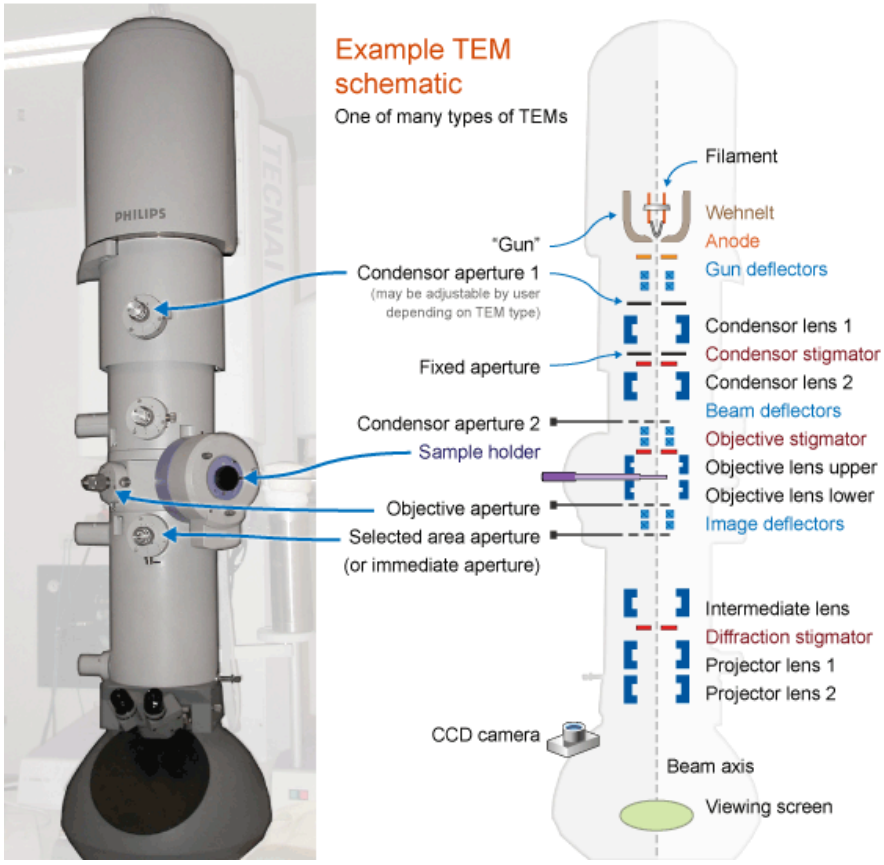

Fig 12: Schematic image of Transmission electron microscope

In the TEM only thin samples, which allow a fraction of the incident electron beam to go through the sample can be studied. When an accelerated beam of electrons impinges upon a sample a rich variety of interactions takes place. Amplitude and phase variations in the transmitted beam provide imaging contrast that is a function of the sample thickness (the amount of material that the electron beam must pass through) and the sample material (heavier atoms scatter more electrons and therefore have a smaller electron mean free path than lighter atoms). Successful imaging of nano-particles using TEM depends on the contrast of the sample relative to the background. Samples are prepared for imaging by drying nano-

particles on a copper grid that is coated with a thin layer of carbon. Materials with electron densities that are significantly higher than amorphous carbon are easily imaged. These materials include most metals (e.g., silver, gold, copper, aluminum), most oxides (e.g., silica, aluminum oxide, titanium oxide), and other particles such as polymer nano-particles, carbon nano-tubes, quantum dots, and magnetic nano-particles.

2.3. Characterization of TGA capped Quantum Dot Doped Liquid Crystal Composites

2.3.1. Material used:

For the present research study, FLC 4327-100 was used. The various physical properties and phase sequence of ferroelectric liquid crystal [18-21] is listed in table given below:

Table 2: Physical properties of liquid crystal

Parameter	Properties
Name	ZLI 4237-100
Phase transition	$Cr \xrightarrow{20^oC} Sm\ C^* \xrightarrow{61^oC} Sm\ A \xrightarrow{73^oC} N^* \xrightarrow{83^oC} Iso$
Pitch(μm)	10
Spontaneous polarization($\frac{nC}{cm^2}$)	20
Tilt angle	24.5^o
Rotantional viscosity(γ)	0.185Pas
Complex Dielectric constant	3.5 to 4.5
Conductivity	$1.3*10^{-9}\Omega^{-1}m^{-1}$

2.3.2. Sample Preparation:

Sample cells were made using two optically flat glass substrates ITO coated. To obtain planar alignment the conducting layer were pretreated by polyamide and then dried in oven for 50min. After that it was rubbed in anti parallel direction with vevlet cloth. The cell thickness was fixed by placing a Mylar spacer (5μm in present study) in between the glass substrate and then sealed with UV sealant (NOA 65). The empty sample cells were calibrated using analytical reagent (AR) grade C_6H_6 (Benzene) as standard references for dielectric study. The Quantum dot LC suspension was prepared by dispersing synthesized CdSe

Methodology

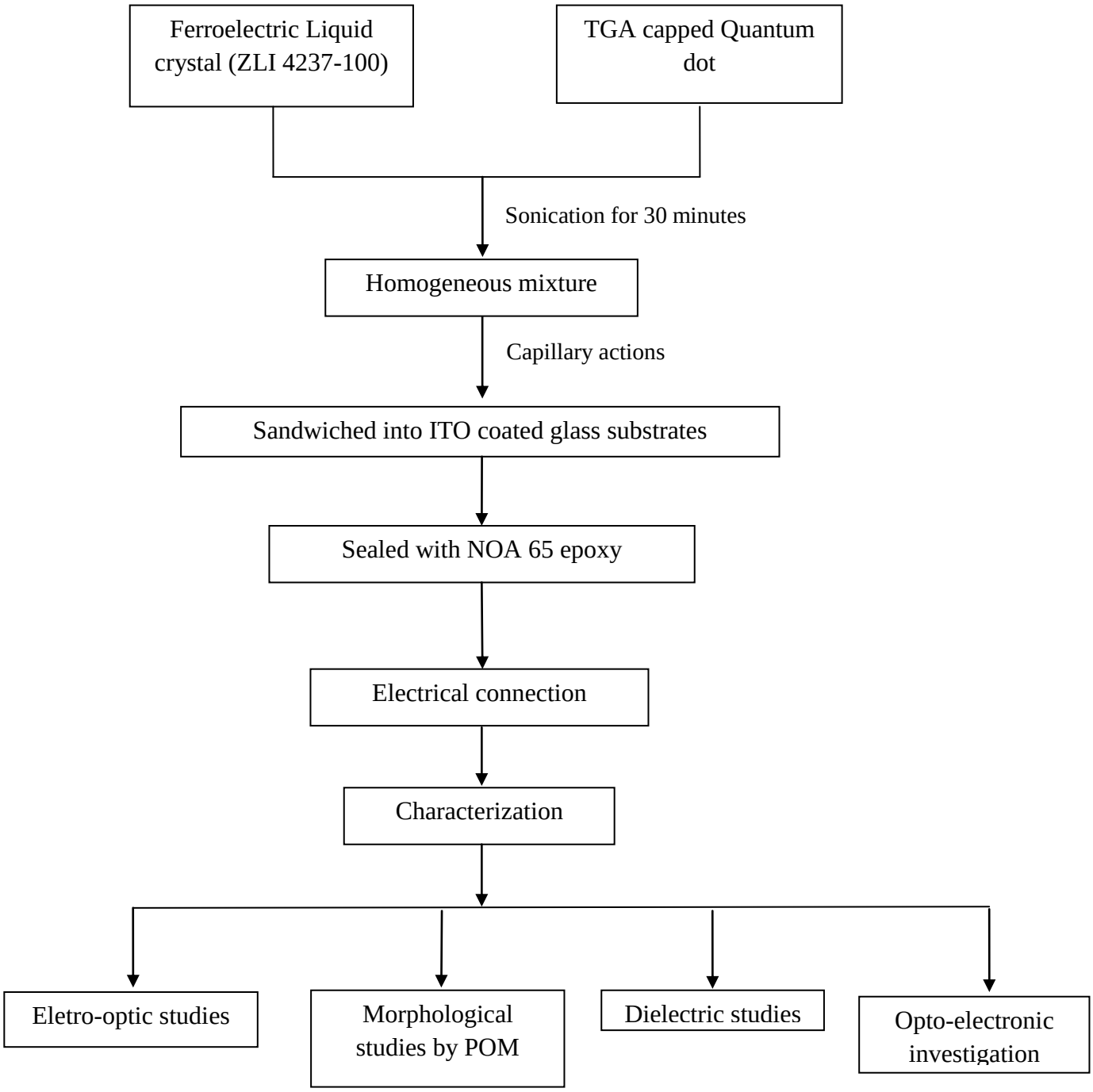

Fig 13: Overall flow chart regarding the preparation of quantum dot liquid crystal cell.

quantum dots with varying concentration from 0.25, 0.5, 1, and 2wt % in the pure FLC(ZLI - 4237-100), purchased by E merck. The assembled cells were filled with the pure and different doped FLC at temperature slightly higher than the isotropic temperature by means of capillary method and then cooled gradually up to room temperature. The alignment of the sample was checked by the polarizing microscope under the crossed polarizer-analyzer arrangement. Overall flow chart regarding the preparation of quantum dot liquid crystal cell is shown in the fig 13[22]

2.4. Analysis for Quantum Dot Doped Liquid Crystal Composite

For the complete analysis of variation in the properties of liquid crystal due to the dispersion of Quantum dot, we have to perform the following studies:

1. Morphological analysis
2. Dielectric analysis
3. Polarization analysis

2.4.1. Morphological Analysis:

Morphology is generally defined as the study of shape, size, texture and phase distribution of physical objects. In liquid crystal, Morphological analysis includes identification of various phases present, study of phase transition, texture analysis, and switching etc. For this analysis we have used Polarizing optical miocroscope from Curl Zeiss (Model Scope A1) with hot Stage (model THMS 2028) connected with temperature controller (model T96-HS) interfaced with computer controlled software Axio vision (Carl Ziess).

The polarized optical microscope is deviced to analyze the specimens that are visible mainly due to their optically anisotropic character. Every microscope generally has four basic components: 1).Eye piece 2). polarizer 3). objective and 4). Analyzer as shown in the fig. 14. Among these polarizer and analyzer are the crucial and basically are optical filters. Polarizer is used to polarized the white light into certain specific direction known as plane polarized light**.** This plane polarized interacts with birefrigent specimen to produce two individual wave components, which are polarized in mutually perpendicular planes. These resulting components have different velocity as well as direction of propagation and are also out of phase. After interaction, these components recombine either by constructive or destructive interference. In the end, these are analyzed by another polarizer known as analyzer. [23-25]

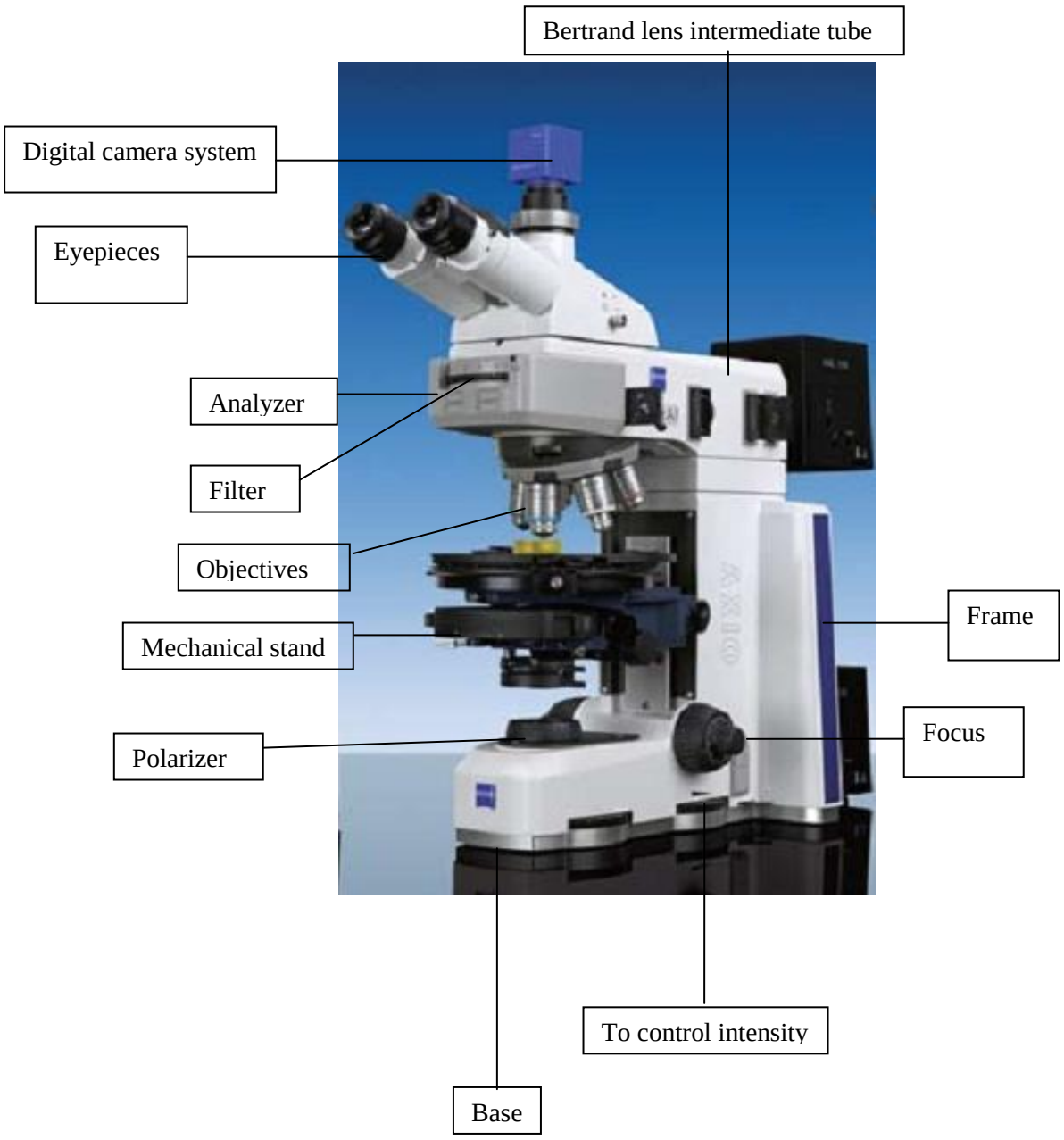

Fig 14: Leveled diagram of polarizing optical microscope

2.4.2. Dielectric Analysis:

A dielectric is generally defined as the electrically insulating material between the metallic plates of a capacitor. An effective dielectric typically contains polar molecules that reorient in external electric field. This dielectric polarization increases the capacitor's capacitance **(**i.e charge storing capacity).

Now, dielectric dispersion is the dependence of the permittivity of a dielectric material on the frequency of an applied electric field. Because there is always a lag between changes in polarization and changes in an electric field, the permittivity of the dielectric is a complicated, complex-valued function of frequency of the electric field. [26-30]

Total dielectric constant = electronic polarization + ionic polarization + orientation polarization + space charge.

Electronic contribution is due to movement of electrons and observed in all frequency. Ionic polarization is due to ions exchange and observed in the frequency range Orientation polarization is due to orientation of dipole and generally observed in the material having fluidity property for example liquid , liquid crystal etc. Space charge polarization is due to interface, grain boundary etc. All these different polarization are shown in the figure15. Out of these contributions electronic polarization is observed in all materials but its contribution is least. In liquid crystal, orientation polarization majorly contributes to dielectric constant. It is very important for the application of dielectric materials and the analysis of polarization systems. Dielectric constant shows characteristic variation with variation of temperature and pressure. Generally dielectric permittivity decreases with increase in temperature and frequency. Some interesting points regarding the dielectric constant variation with frequency are listed. When the frequency becomes higher:

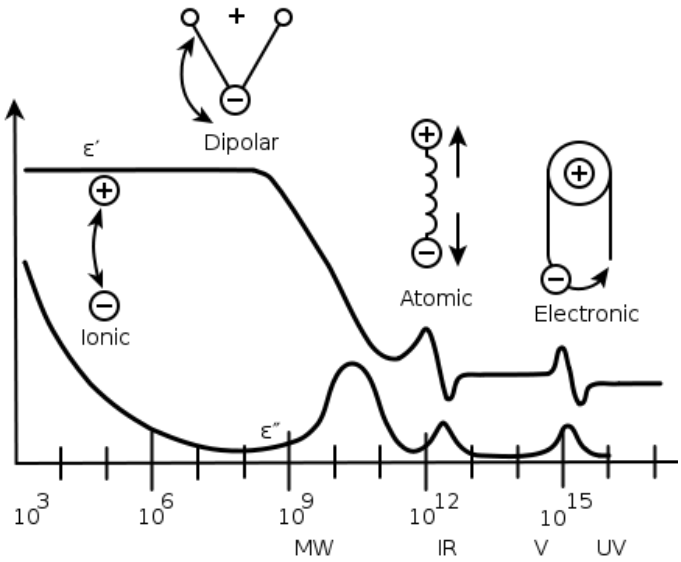

Fig 15: Different types of polarization

- it becomes impossible for dipolar polarization to follow the electric field in the microwave region around 10^{10} Hz;
- in the infrared or far-infrared region around 10^{13} Hz, ionic polarization loses the response to the electric field;
- Electronic polarization loses its response in the ultraviolet region around 10^{15} Hz.

Fig 16: Programmable RCL meter [Model- FLUKE PM6306] for dielectric analysis

In the wavelength region below ultraviolet, permittivity approaches the constant ε_0 in every substance, where ε_0 is the permittivity of the free space. Because permittivity indicates the strength of the relation between an electric field and polarization, if a polarization process loses its response, permittivity decreases.[27-30]

In brief decrease in the dielectric constant is due to increase in the randomizations of dipole. This further leads to an increase in the entropy of the system. This leads to increase in instability. So, dipole in liquid crystal tries to return to their mean position. But this process consumes time. This overall phenomenon is known as relaxation process. For these analysis of dielectric constant of liquid crystal composite we have used RCL meter having model no.PM 6306 having frequency range up to from 50Hz to 1MHz, which is shown in the fig. 16.

References:

1. N. Gaponik, D. V. Talapin, A. L. Rogach, K. Hoppe, E. V. Shevchenko, A. Kornowski, A. Eychmu1ller, & H. Weller, "Thiol-Capping of CdTe Nanocrystals: An Alternative to Organometallic Synthetic Routes" Journal of Physical Chemistry B, **106** (2002) 7177-7185.
2. W Mi, J. Tian, W. Tian, J. Dai, X. Wang & X. Liu "Temperature dependent synthesis and optical properties of CdSe quantum dots" Ceramics international **38** (2012) 5575-5583.
3. M. Green"The nature of quantum dots capping ligands", Journal of materials Chemistry, **20** (2010) 5797- 5809.
4. Y. Yin & A. P. Alivisatos,"Colloidal nanocrystal synthesis and the organic–inorganic interface" Nature, **437** (2005) 664-670.
5. Z. A. Peng & X. Peng "Nearly Monodisperse and Shape-Controlled CdSe Nanocrystals via Alternative Routes: Nucleation and Growth" Journal of Americian Chemical. Society, **124** (2002) 3343-3353.
6. Z. A. Peng & X. Peng "Nearly Monodisperse and Shape-Controlled CdSe Nanocrystals via Alternative Routes: Nucleation and Growth" Journal of Americian Chemical. Society, **124** (2002) 3343-3353.
7. X. Peng "Mechanism for the shape control and shape evolution of colloidal semiconductor nanocrystals", Advanced materials, **15** (2003) 459-463.
8. Q. Sun, S. Fu, T. Dong, S. Liu & C. Huang "Aqueous Synthesis and Characterization of TGA-capped CdSe Quantum Dots at Freezing Temperature" Molecules, **17** (2012) 8430-8438.
9. R. Zhang, A. Khalizov, L. Wang, M. Hu, & W. Xu, "Nucleation and Growth of Nanoparticles in the Atmosphere", Chemical review, dx.doi.org/10.1021/cr2001756.
10. C. Baudot, C. M. Tanb, & J. C. Konga, "FTIR spectroscopy as a tool for nano-material characterization", Infrared Physics & Technology **53** (2010) 434–438.
11. D. L. Schodek, P. Ferreira and M. F. Ashby "Nanomaterials, nanotechnologies and design: an introduction for engineers",Butterworth Hiemann, (2009) 287-290.
12. R. B. Vasiliev, V. S. Vinogradov, S. G. Dorofeev, S. P. Kozyrev, I. V. Kucherenko & N. N. Novikova, "IR-active vibrational modes of CdTe, CdSe, and CdTe/CdSe colloidal quantum dot ensembles", Journal of Physics: Conference Series **92** (2007) 012054.
13. J. K. Cooper, A. M. Franco, S. Gul, C. Corrado, & J. Z. Zhang, "Characterization of primary amine capped CdSe, ZnSe and ZnS quantum dots by FTIR : determination of surface bonding interaction and identification of selective desorption", Langmuir, **27** (2011) 8486–8493.
14. P. Srivastava & K. Singh, "Synthesis of CdSe nanoparticles by solvothermal route: Structural, optical and spectroscopic properties" Advanced Materials Letters, **3** (2012) 340-344.
15. V. Amendola & M. Meneghetti," Size Evaluation of Gold Nanoparticles by UV-vis Spectroscopy", Journal of Physical Chemistry C, **113 (2009)** 4277–428.

16. S. J. Rosenthal, J. McBride, S. J. Pennycook, L. C. Feldman, "Synthesis, surface studies, composition and structural characterization of CdSe, core/shell and biologically active nanocrystals" Surface Science Reports **62** (2007) 111–157.
17. A. Oudhia "UV-VIS spectroscopy as a nondestructive and effective characterization tool for II-VI Compounds" Recent Research in Science and Technology **4(8)** (2012) 109-111.
18. C.N.R. Rao & K. Biswas ,"Characterization of Nanomaterials by Physical Methods", Annual review of analytical chemistry **2** (2009) 435–462.
19. M. Ghosh, E.V. Sampathkumaran, C.N.R. Rao., "Synthesis and magnetic property of CoO nanocrystals" Chemistry of Materials **16** (2005) 2348–2352.
20. W.W. Yu, L. Qu, W. Guo, X. Peng "Experimental determination of the extinction coefficient of CdTe, CdSe, and CdS nanocrystals", Chemistry of materials **15** (2003) 2854–60.
21. S. Iijima, T. Ichihashi "Single-shell carbon nanotubes of 1-nm diameter". Nature **363** (1993) 603–605.
22. S. Iijima "Helical microtubules of graphitic carbon" Nature **354** (1991) 56–58.
23. C.B. Murray, C.R. Kagan, M.G. Bawendi "Synthesis and characterization of monodisperse nanocrystals and close-packed nanocrystal assembly", Annual Review of Materials Science **30** (2000) 545–610.
24. P. Malik, K. K. Raina, A. Bubnov, A. Chaudharya & R. Singh "Electro-optic switching and dielectric spectroscopy studies of ferroelectric liquid crystal crystals with low and high spontaneous polarization" Thin solid films **519** (2010) 1052-1055
25. S. Khosla & K. K. Raina, "Switching responses of Ferroelectric liquid crystals" Indian journal of Pure & applied Physics, 42 (2004) 49 - 45.
26. C. Langer & R. Stannarius "Travelling Polarization walls In Freely Suspended Smectic C* films" Ferroelectrics **244** (2000) 347.
27. P. Arora, A. Mikulko, F. Podgornov, & W. Haase "Dielectric and Electro-Optic Properties of New Ferroelectric Liquid Crystalline Mixture Doped with Carbon Nanotubes" Molecular Crystals and Liquid Crystals, 502 (2009) 1.
28. A. K. Misra, A. K. Srivastava, J. P. Shukla, & R. Manohar "Dielectric and electro-optical parameters of two ferroelectric liquid crystals: a comparative study" Physica Scripta **78** (2008) 065602
29. D. P. Singh, S. K. Gupta, A. C. Pandey & R. Manohar "Dielectric relaxation and electrical properties of ZnO1-xSx nanoparticle dispersed ferroelectric mesophase" Advanced Materials Letters (2013) **4 (**2013) 556-561.
30. H.J. Coles, H.F. Glesson, & J. S. Kang,"Dye guest host effects in ferroelectric liquid-crystals". Liquid Crystal **5** (1989) 1243–1252.
31. P. Arora, A. Mikulko, F. Podgornov, & W. Hasse, "Dielectric and electro-optical properties of new ferroelectric liquid crystalline mixture doped with carbon nanotube" Molecular Crystal Liquid Crystal **502** (2009) 1–8.

Chapter 3: Results and Discussion

3.1. Characterization of TGA Capped CdSe Quantum Dot

3.1.1. FTIR Analysis:

FTIR spectrum of the TGA capped CdSe quantum dot is shown in the figure 1. The peaks at 1380 cm^{-1} are due to shifting of asymmetrical vibration of carboxylic group of in TGA. The peak at 1672 cm^{-1} corresponds to the co stretching of carboxylic group. The peaks around 2969 and 3225 cm^{-1} are due to sp^3 stretching of C-H and due to vibration of O-H group present in TGA. There is shifting of S-H group peak from 2560 cm^{-1} to 2342cm^{-1}, this may be attributed to formation of S-Cd bonds[1-5] between thioglycolic acid (TGA) and CdSe as shown in the figure 2, which confirms the TGA capping on the CdSe quantum dots.[1-4]

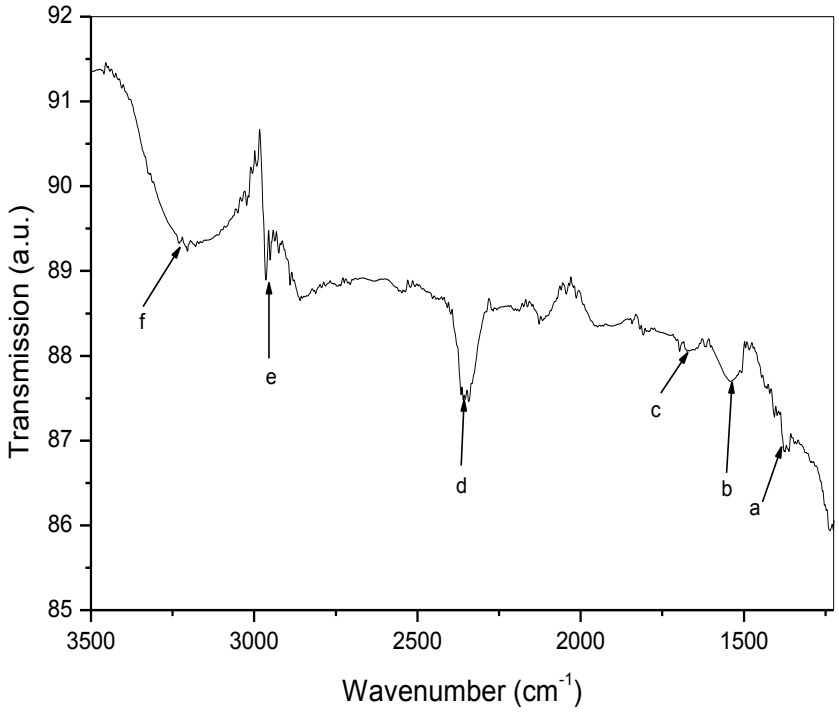

Fig 1: FTIR spectra of TGA capped CdSe quantum dot

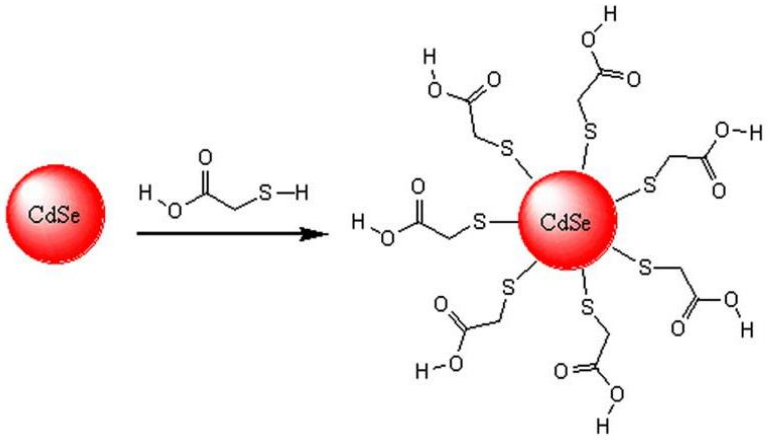

Fig 2: Pictorial representation of chemical reaction for the preparation of TGA capped CdSe quantum dot

Table 1: various peaks present in the FTIR spectra

	Wave-number (cm^{-1})	**Peaks and their details**
A	1380	Shifting of asymmetric vibration of carboxylic group in TGA
B	1533	
C	1672	C=O stretching of carboxylic group.
D	2342	S-H peak from 2560cm^{-1} to 2342 cm^{-1}.
D	2969	Sp^3 stretching of C-H
f	3225	Broad absorption band around 3400 cm^{-1} was assigned to O-H vibration of the absorbed COOH

3.1.2. Photo-Luminescence Analysis:

The growth of CdSe quantum dots have investigated with the help of fluorescence spectrophotometer from Agilent technology (Model Cary Eclipse Fluorescence Spectrophotometer). The excitation and emission slit size [6-8] is kept constant at 5nm during the whole set of experiment. As we raise the reaction temperature 55^{o}C to 85^{o}C, TGA capped CdSe quantum dots solution is taken out from the three neck flask at 55^{o}C, 65^{o}C, 70^{o}C and 85^{o}C. To investigate the formation of CdSe quantum dots, we compare the fluorescence spectra of all samples which is shown in the fig. 3. The excitation and emission spectra shows clearly the effect on growth of CdSe quantum dot. The various parameters like Stoke shift and quantum yield listed in the Table 1 & 2 can be controlled as a function of reaction temperature. The Stoke shift is calculated by the difference between emission and excitation wavelength of quantum dots. The shape of excitation spectra in fig. [1(b-c)] is not exactly as gaussian fitted, which represents the asymmetry in the excitation spectrum. But this asymmetry is getting controlled as we raise the reaction temperature upto 85^{o}C fig.1 (d) and the maximum excitation wavelength get red shifted from 419.9 nm to 488.96 nm with the increase in reaction temperature from 55^{o}C to 85^{o}C. This clearly reflects the change in energy band gap with change in shape and size of the growth CdSe quantum dots [5-7]. Quantum yield of the sample a to d was calculated with the help of flouroscence spectroscopy as a function of reaction temperature from the spectrum shown in the fig. 3 by the formulae

$$\text{Quantum yield} = \frac{\text{Number of emitted photons}}{\text{number of excitted photons}}$$

As shown in figure 3(a), Fluorescence intensity in excitation spectra is very high as compare to emission which represents low quantum yield. But as we raise the temperature, the PL intensity of excitation and emission beam comparable (in fig3 (b-c)). On further raise to the temperature at 85^{o}C, number of photons excited become less than as compared to numbers of photons emitted as shown in figure 3(d), which suggestes, there is increase in quantum yield as describes in table 1. This effect is clearly visible in the image taken during the synthesis of CdSe quantum dots shown in the fig. 4.

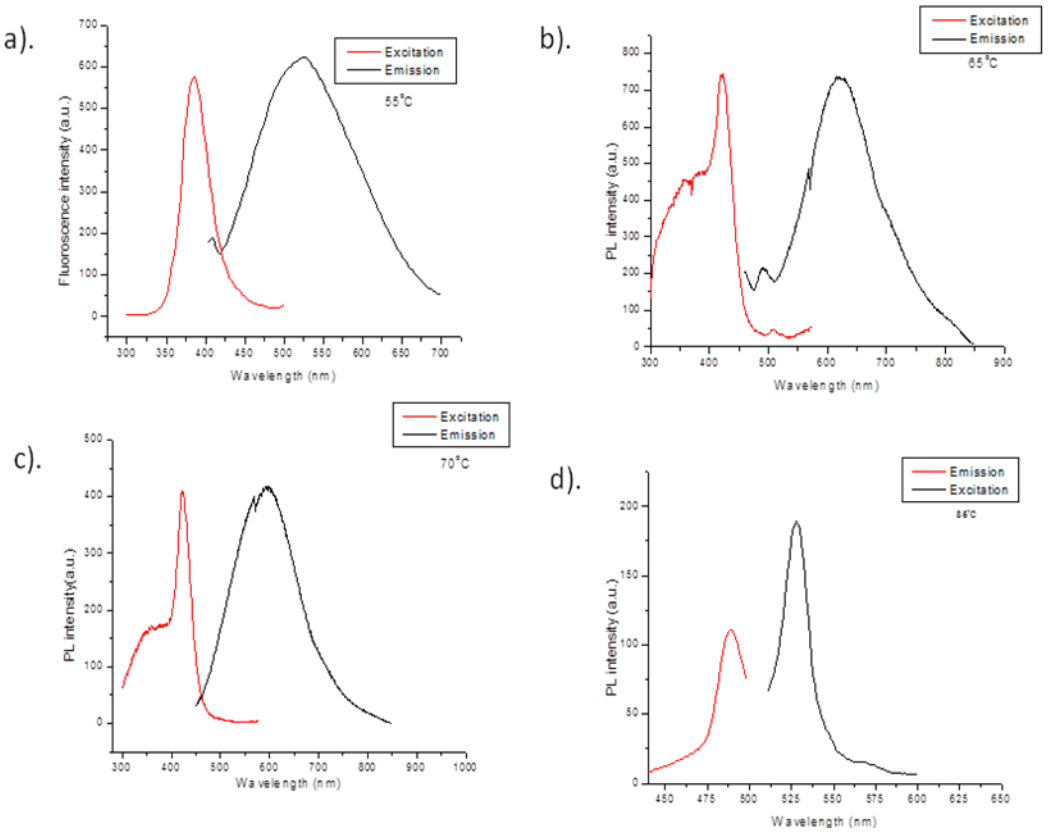

Fig 3: Emission and excitation spectra of TGA capped CdSe quantum dot at different synthesis temperature a) 55^{O}C, b) 65^{O}C, c) 70^{O}C, and d) 85^{O}C

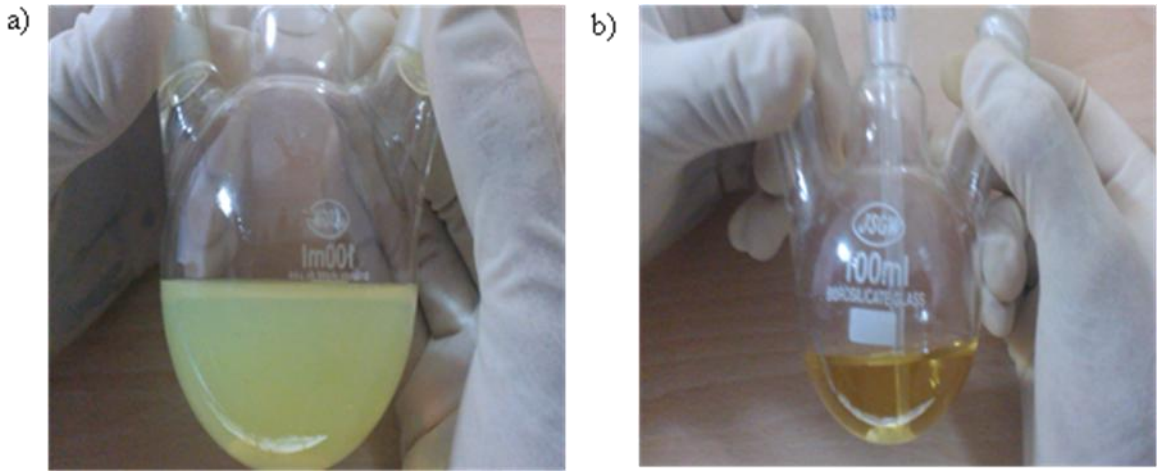

Fig 4: Image of enhanced quantum yield of CdSe quantum dots taken during the experiment

Table 1: various parameters measured at different temperature regarding the TGA capped CdSe quantum dot

Sr. No.	Temperature (^oC)	λ_{ex} (nm)	λ_{em} (nm)	Stoke Shift (nm)	PL intensity at λ_{ex} (a.u.)	PL intensity at λ_{em} (a.u.)	Quantum yield
1	55	419.9	547.17	127.27	946.56	603.28	0.63734
2	65	421.17	621.37	200.2	740.20	730.86	0.98738
3	70	422.42	596.23	173.81	409.39	417.04	1.01869
4	85	488.96	528.54	39.58	110.098	188.102	1.708496

Table 2: Emission and excitation parameters measured regarding TGA capped quantum dot

Temperature (^oC)	Excitation (Gaussian fitting)		Emission (Gaussian fitting)	
	FWHM (nm)	Peak Centre λ_{ex} (nm)	FWHM (nm)	Peak Centreλ_{em}(nm)
55	64.762	417.61	120.34	553.88
65	106.01	424.91	120.92	624.56
70	38.28	419.96	131.33	591.65
85	17.575	489.78	17.744	527.12

3.1.3. UV Vis Spectroscopy:

Fig.5 shows the UV- Vis spectra of TGA capped CdSe quantum dots for the optimization of pH value. At pH =8, there is no peak found in the wavelength range [8-13] 350-550 nm. Whereas at pH = 10 absorption peak is found at 385nm which matches to reported literature

values [ref.]. It gives the confirmation of CdSe quantum dots hence the energy band gap is calculated here by using formulae.

$$E = \frac{hc}{\lambda_{cut\ off}}$$

Where as $\lambda_{cut\ off}$ is the cut off wavelength to calculate the band gap energy which is found to be 2.37 eV [referance]. On the contrary, the band gap energy of bulk CdSe is 1.8 eV[referance].

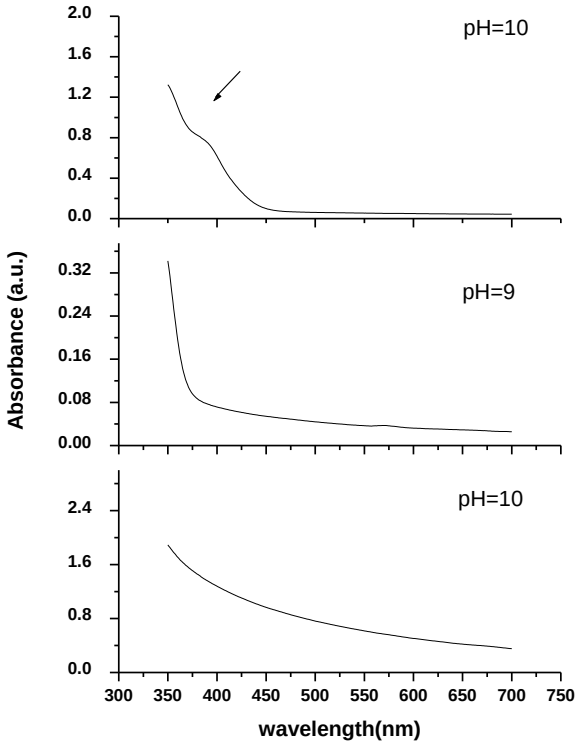

Fig 5: UV-Vis spectra of TGA capped CdSe quantum dot as function of pH

3.1.4 TEM Analysis

In order to further investigate the particle morphology and size of particle in TGA capped CdSe quantum dot, TEM image was taken and is as shown in Figure 6. For the analysis of TEM, specimen was prepared by dispersing synthesized CdSe quantum dot in ethanol and then well sonicated ultra-sonicately. The particles were picked up using carbon coated copper grid and examined. The TEM instrument was [13-15] equipped with a

system performing SAED to further characterize nanostructure of powder. The TEM image confirms that the average particle size is 6-7 nm, spherical in shape and are polycrystalline in nature [fig. 6(d)]; which is confirmed by the circular bright continuous rings in the SAED pattern corroborate. [16-17]

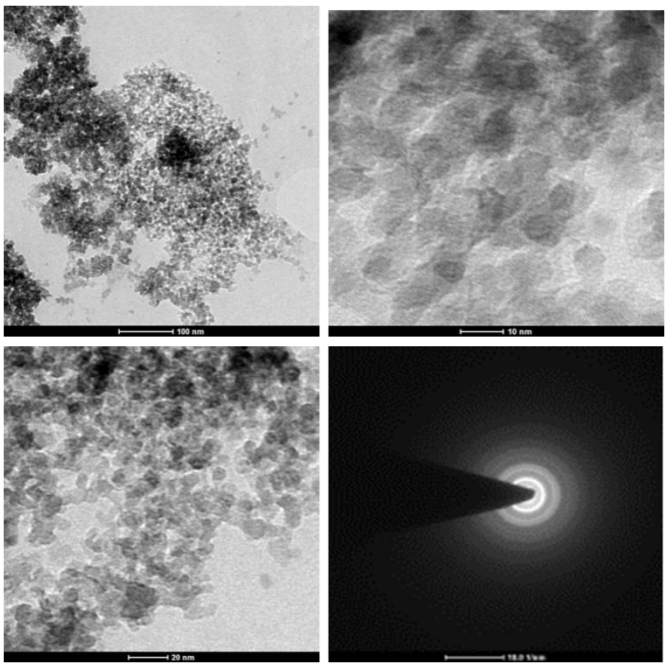

Fig 6: TEM imaging of CdSe quantum dot.

3.2 TGA Capped CdSe Quantum Dot Doped Ferroelectric Liquid Crystal: [18-21]

3.2.1 Morphological Investigation by Polarization Optical Microscope:

Fig. 7(a) shows that bookself geometry in pure ferroelectric liquid crystal (ZLI 4237-100), which have chiral Sm C* phase, having pitch (p) 10μm. As the pitch (p) is greater than cell thickness (d), so the ferroelectric liquid crystal molecules are getting suppressed by the pretreated polymide coated conducting (ITO) surface. Hence the idealized bookself texture appears with symmetrical zig zag effects (shown in fig. 7(a). But the dispersion of CdSe quantum dots in ferroelectric liquid crystal creates more surface stabilized domains, [appears in yellow color in texture (a-d)], which improves the optical stability by enhancing the stabilized ferroelectric domains upto the concentration of 1 wt% CdSe quantum dots. But as

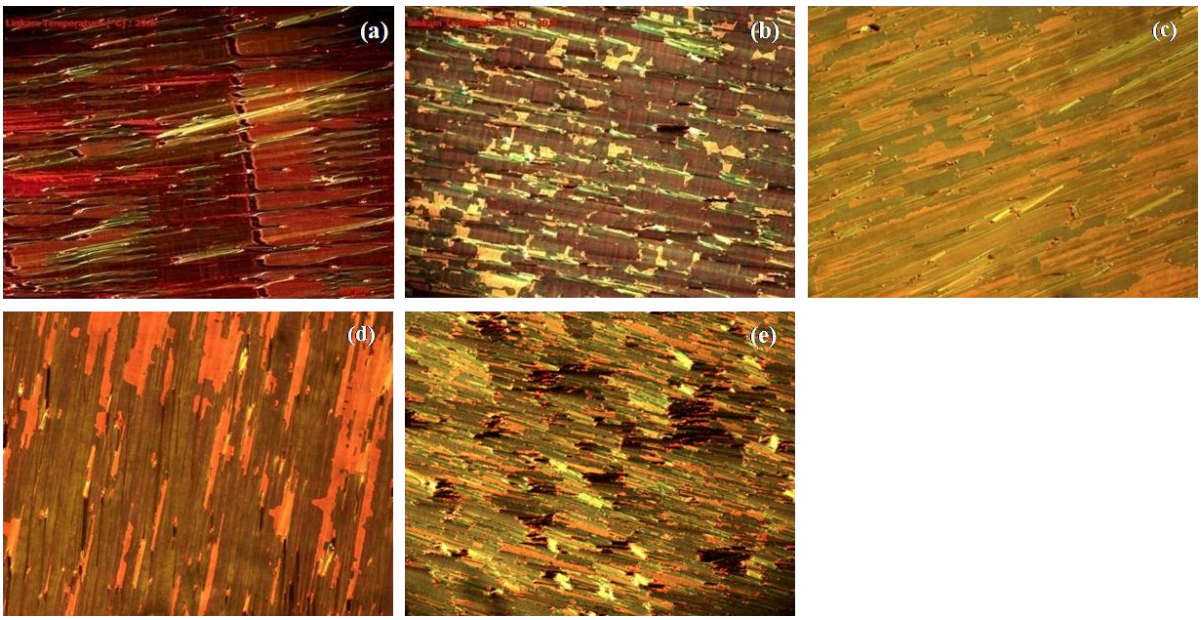

Fig 7: Optical texture of CdSe quantum dot doped Ferroelectric liquid crystal dot.at various concentration of CdSe quantum dots (a) 0% (b) 0.25% (c) 0.5% (d) 1% (e) 2%

we raise the concentration of CdSe quantum dot further upto 2 wt%, these domains gets disappear due to more hindrance of CdSe quantum dots in ferroelectric liquid crystal. Hence, this may cause decrease in the dielectric as well as optical properties.

3.2.2. Molecular Relaxation Phenomenon in CdSe Doped FLC:

The dielectric spectroscopy is a useful tool to investigate the relaxation processes, which arises due to the rotational fluctuations of the molecular dipoles. In the SmC* phase (or ferroelectric phase), chiral FLC molecule are tilted by an angle θ to the director. Two types of fluctuations are possible in this situation i.e. along the phase angle (Φ) and tilt angle (θ). These two fluctuation result in the appearance of the Goldstone mode (GM) and the Soft mode (SM) respectively due to molecular relaxation phenomenon. In the present investigation, we have observed the phase angle fluctuation near 100 Hz, which is analogous to Goldstone relaxation mode. The soft mode was absent in the entire SmC* phase and also near the SmC*-SmA phase transition temperature. The real part of permittivity in SmC* phase is the highest, which identifies the maximum helix strength in the FLC sample. It decreases sharply near SmC* to SmA phase transition because helix starts unwinding. Real part (ϵ^1) of dielectric permittivity shows 11.3%than pure liquid crystal an increase for the concentration (0.25%) of Q.D dispersed in the liquid crystal upto frequency range 100 Hz as

shown in the fig. 6. With the increase in frequency, Real part (ϵ^1) decreases due to effect of different polarization phenomenon with frequency. This trend is shown by all conc. This may be due to the reason that at low frequency dipole can easily aligned in the direction of electric field (applied) and is given by the relation

$$P \propto E$$

Where P is the polarization and E is the electric field.

As we further increase the frequency it becomes very difficult for the dipole to follow (or get aligned) in the direction of electric field. So with increase in frequency, the real part ϵ^1 starts decreasing as very less number of dipole can align.

For the imaginary part of the dielectric permittivity, two peaks are found [shown in fig. 8]. It corresponds to relaxation mode (soft mode, goldstone mode, ITO mode etc) presents. The first corresponds to Goldstone mode (GM) and the second mode signifies the ITO mode, present due to high conduction phenomenon of ITO surface. For first hump observed in the ϵ^{11}graph, relaxation phenomena are responsible. Here molecules are in higher energy unstable). So in order to attain stability molecule starts returning to the state of minimum energy (i.e equilibrium state). But this process consumes certain amount of time interval. For the higher concentration of quantum dot (i.e from 0.5% to 2%) real part of dielectric permittivity shows no significant variation than pure LC. This may be due to the agglomeration or aggregation of CdSe Quantum dot in Ferroelectric Liquid Crystal (FLC) matrix. With increase in concentration of the quantum dot, they hindered the motion of dipole moment and hence have to do more work in order to get align in the direction of electric field. The overall dielectric permittivity can be understood by the formulae:

$$\epsilon^* = \epsilon^1 - \epsilon^{11}$$

As from the fig. 9, we can see that even though there is not much increase in the real part of dielectric permittivity. But there is sufficient decrease in the imaginary. Hence it enhances the overall dielectric properties of the system.

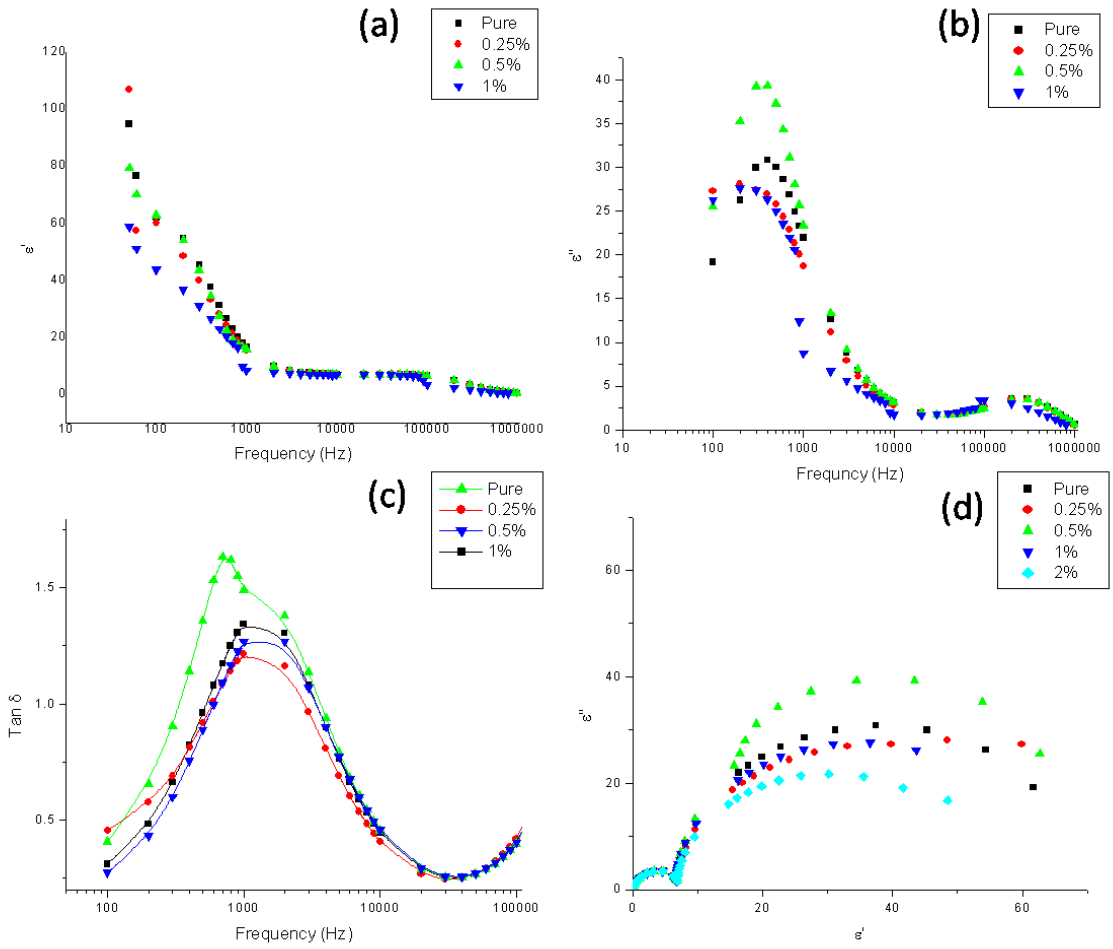

Fig. 8. Dielectric properties- (a): Real part (b) Imaginary part of relative permitivity (c) loss tangent (d) Cole- Cole plot of CdSe quantum dots doped FLC as a function of various concentration of CdSe quantum dots

Temperature dependence of dielectric properties of dielectric properties of 0, 0.25, 0.5,1 weight % CdSe doped FLC was investigated.The temperature dependent behavior show the different phase transition behavior. The Real part (ϵ^1) of dielectric permittivity has maximum value has maximum value in Sm C* phase and the minimum value shows the N*phase present in the CdSe quantum dots doped FLC composites. Hence it is clearly observed from the graph that dielectric properties of CdSe quantum dot doped FLC are influenced by temperature and gives the information about the phase presents in the liquid crystal. The peak shifting to higher frequency [fig.8] shows the fastest relaxation of CdSe doped FLC molecules with raise in temperature.

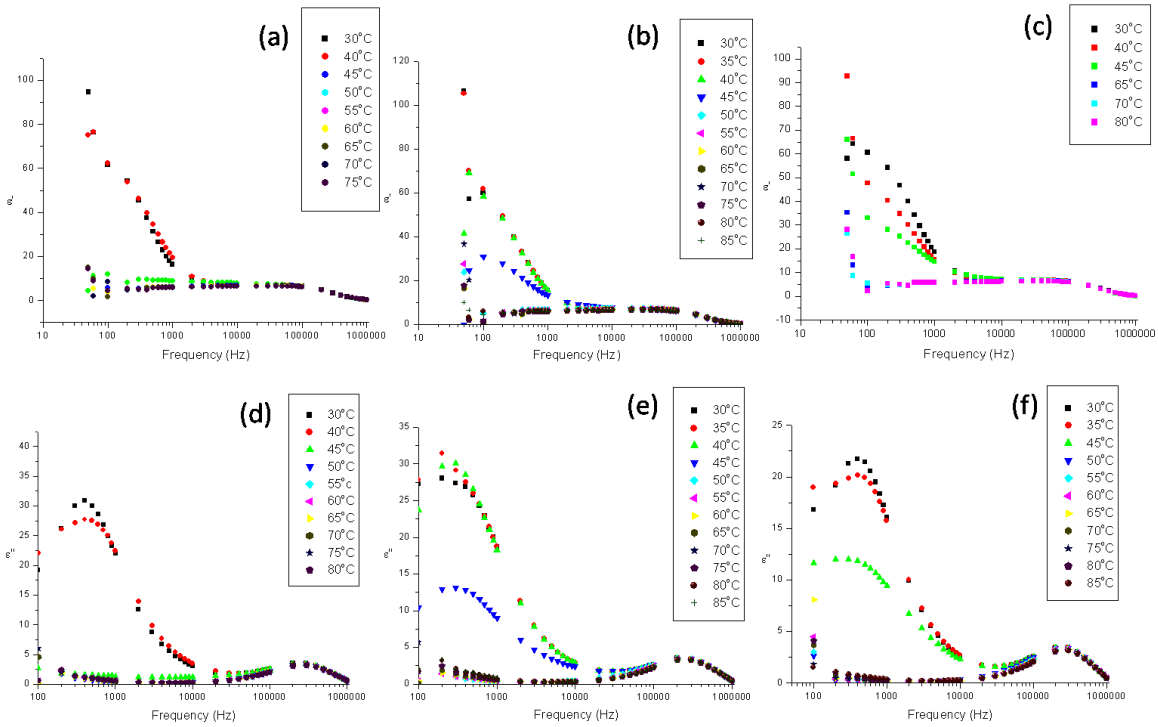

Fig. 9.: Temperature dependence of dielectric properties in real (a,b,c) and imaginary (d,e,f) part of dielectric permittivity in pure , o.25 and 2 wt% CdSe doped FLC composites

3.2.3. Electro-Optic Polarization Switching and Response Time:

Spontaneous Polarization and Response time of CdSe quantum dots By this we measure the current peak in the overall current response with the application of triangular wave The experimental set up of the electro-optic polarization switching is shown in the fig.10. The triangular and square wave pulses were applied to the cells through Function generator (HCL, Model HIL2821). The current and voltage pulses were detected on a Digitizing storage oscilloscope (TEKTRONIX TDS210 having 1GS/s sample rate and 60 MHz bandwidth) across 100 kΩ standerd resistor. The whole set up was interfaced with computer (PENTIUM-II) for data acquisition and analysis was done using done wave star software and the output response collected in software is shown in the fig.11. In order to study the molecular re-orientation processes associated with the helix dynamics, the symmetric -10V-0V- +10V ($20V_{pp}$), the square and triangular wave pulses were applied to the sample cells. The symmetric triangular or square wave pulses to CdSe doped FLC mixture reorients the dipoles between two stable polarization states (Up and Down). As the field is switched on,

molecular alignment in the form of voltage drop is detected on the storage oscilloscope. [shown in fig. 11]

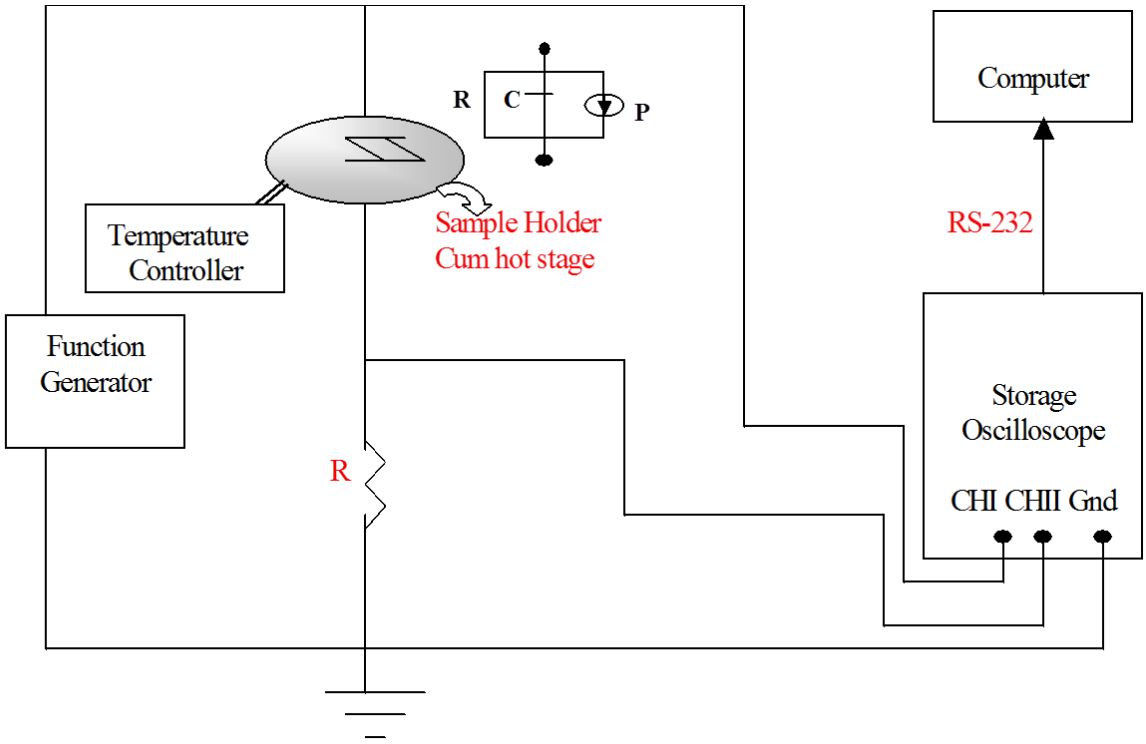

Fig 10: Electro-optic setup for measurement of polarization by polarization reversal

In SmC* phase for certain applied voltage V, the current (I) response consists of three components:

1). The capacitive term I_c 2). The ionic conduction term I_R 3). Polarization current I_P

Thus total measured output current I(t) across the standard resistor R can be written as:

$$I=I_R+I_C+I_P=\frac{V(t)}{R}+C\frac{dV(t)}{dt}+a_s\frac{dP_s}{dt}$$

Whereas $C=\frac{\epsilon_\perp * \epsilon_a * a_S}{d_s}$ is the capacity of a cell; d_s, a_s and R are the thickness, area and resistance of the cell respectively. V (t) is the voltage across the cell.

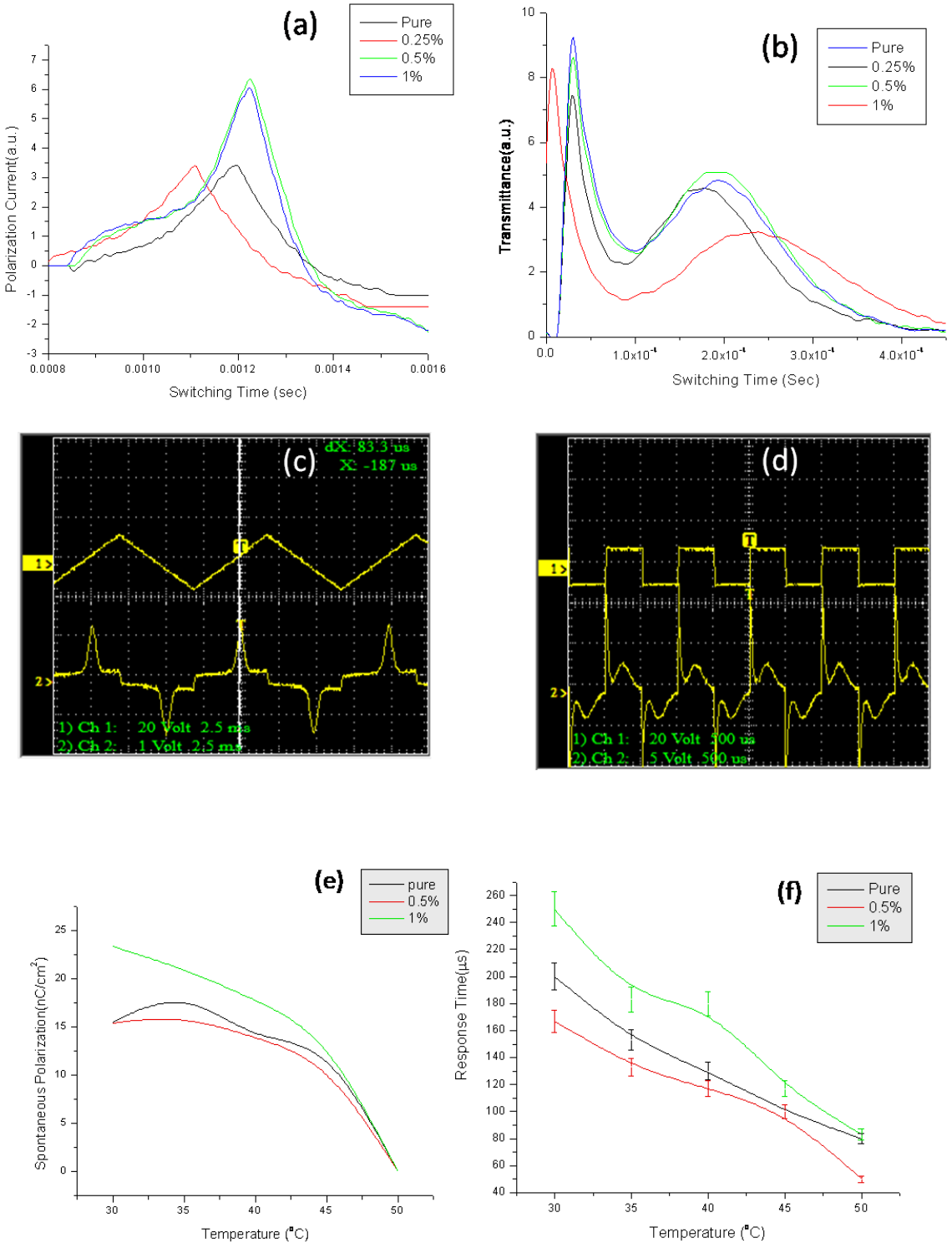

Fig 11: Capture of input and output response of polarization current measurement in (a, c and e) spontaneous polarization measurement during application of triangular wave (b, d and f). Response time measurement during application of response wave pulse in CdSe doped FLC composites

We observed that polarization enhances in 0.5% CdSe doped FLC composite than pure FLC whereas response time decreases 19% from the pure FLC in case of 1% CdSe doped FLC which slows down the switching of FLC molecules due to highest hinderance of CdSe quantum dot But in case of 0.25% CdSe doped FLC response time decreases upto 20% than pure which improve the switching response of FLC.

References :

1. J. K. Cooper, A. M. Franco, S. Gul, C. Corrado, & J. Z. Zhang "Characterization of Primary Amine Capped CdSe, ZnSe, and ZnS Quantum Dots by FT-IR: Determination of Surface Bonding Interaction and Identification of Selective Desorption", Langmuir, **27** (2011) 8486–8493.
2. R B Vasiliev, V S Vinogradov, S G Dorofeev, S P Kozyrev, I V Kucherenko & N N Novikova "IR-active vibrational modes of CdTe, CdSe, and CdTe/CdSe colloidal quantum dot ensembles" Journal of Physics: Conference Series **92** (2007) 012054.
3. J. Peng, S. Liu, L. Wang, Z. Liu & Y. He "Study on the interaction between CdSe quantum dots and chitosan by scattering spectra" Journal of Colloid and Interface Science 338 (2009) 578–583
4. S. Sinha, S. K. Chatterjee, J. Ghosh, & A. K. Meikap "Structural characterization and observation of variable range hopping conduction mechanism at high temperature in CdSe quantum dot solids" Journal of applied physics **113** (2013) 093703.
5. L. Li, H. Qian, N. Fang & J. Ren "Significant enhancement of the quantum yield of CdTe nanocrystals synthesized in aqueous phase by controlling the pH and concentrations of precursor solutions" Journal of Luminescence **116** (2006) 59–66.
6. B. Kinkead & T. Hegmann, "Effects of size, Capping agent, and concentration of CdSe and CdTe quantum dots doped into a nematic liquid crystal on the optical and electro-optic properties of the final collidal liquid crysdtal mixture ", Journal of Material chemistry **20** (2010) 448-458.
7. W. Mi, J. Tian, J. Jia, W. Tian, J. Dai & X.Wang "Characterization of nucleation and growth kinetics of the formation of water soluble CdSe quantum, dots by their optical properties", Journal of Physics D: Applied Phyics **45** (2012) 435303.
8. B. Pan, D. Cui, R. He, F. Gao & Y. Zhang "Covalent attachment of quantum dot on carbon nanotubes" Chemical Physics Letters **417** (2006) 419–424.
9. Y. Wang, J. P. Lu & Z. F. Tong "Rapid synthesis of CdSe nanocrystals in aqueous solution at room temperature" Bulletin of Materials Science **33** (2010) 543–546.

10. A. Wolcott, D. Gerion, M. Visconte, J. Sun, A. Schwartzberg, S. Chen, & J. Z. Zhang, "Silica-Coated CdTe Quantum Dots Functionalized with Thiols for Bioconjugation to IgG Proteins" Journal Physics Chemistry B **110** (2006) 5779-5789.
11. S. K. Mehta, Savita Chaudhary, Sanjay Kumar, & Sukhjinder Singh "Facile synthesis, growth mechanism, and optical properties of CdSe nanoparticles in self-assembled micellar media and their efficient conjugation with proteins", Journal of Nanoparticle Research **12** (2010) 1697–1709.
12. C. Tuinenga, J. Jasinski,T. Iwamoto, & V. Chikan "In Situ Observation of Heterogeneous Growth of CdSe Quantum Dots: Effect of Indium Doping on the Growth Kinetics" Nano **2** (2008) 1411–1421.
13. F. Aldeek, L Balan, J. Lambert & R. Schneider "The influence of capping thioalkyl acid on the growth and photoluminescence efficiency of CdTe and CdSe quantum dots", Nanotechnology **19** (2008) 475401.
14. S. Neeleshwar, C.L.Chen, C.B.Tsai, & Y.Y.chen, "Size dependent properties of CdSe quantum dots", Physical Review B **71** (2005) 201307-1.
15. B. Suo, X. Su,J. Wu, D. Chen, A. Wang & Z. Guo "Poly (vinyl alcohol) thin film filled with CdSe–ZnS quantum dots: Fabrication, characterization and optical properties" Materials Chemistry and Physics1**19** (2010) 237–242.
16. S. K. Gupta, D.P.Singh, P. K. Tripathi, R. Manohar, M. Varia, L. K. sagar & S. Kumar, "Regarding the liquid crystal CdSe quantum dot dispersed DOBAMBC: an electro-optic study" Liquid crystals, (2013).
17. A. Kumar, P. Silotia & A. M. Biradar, "sign reversal of dielectric of ferroelectric of ferroelectric liquid crystals doped with Cadmium Telluride quantum dots", Applied Physics Letters, **99** (2011) 072902.
18. X. Tong & Y Zhao, "Liquid crystal gel dispersed quantum dots: Reversible Modulation of Photoluminescence intensity using an electric field", Journal of American Chemistry Society, **129** (2007) 6372-6373.
19. J. Mirzaei, M. Urbanski, K. Yu, H. S. Kitzerow & T. Hegmann "Nanocomposites of a nematic liquid crystal doped with magic-sized CdSe quantum dots" Journal of Materials Chemistry, **21** (2011) 12710.

Chapter 4: Conclusions and Future Scope

We have successfully synthesized the CdSe quantum dot with high quantum yield at optimized reaction condition such as reaction temperature 85^{o}C for 10 hours and prepared cadmium and selenium source heaving Cd^{2+}: Se: TGA is 0.035:0.01:0.07 at adjustable pH=10 of the solution.

Then the final product of fluorescent TGA quantum CdSe quantum dots are characterized as

- TEM studies show that the size of spherical TGA capped CdSe quantum dots is 7nm.
- FTIR spectroscopy confirms the chemical bonding and TGA capping on the CdSe quantum dots.
- UV-Vis confirm the band gap of TGA capped CdSe quantum dots increases upto 2.37 eV due to quantum confinement on CdSe nanocrystals whereas the band gap of bulk CdSe is 1.8 eV
- PL spectroscopy confirms the yellow emission corresponding to 528nm wavelength with high quantum yield value in different set of experiments.

The molecular relaxation phenomenon of CdSe doped FLC composite was investigated as

- Real part (ϵ') of dielectric permittivity of 0.25% CdSe doped FLC improves 11% than the undoped ferroelectric liquid crystal whereas at higher concentration 1% of CdSe quantum dot, dielectric permivitivity decreases due to agglomeration or aggregation of CdSe quantum dots in FLC matrix.
- Imaginary part (ϵ'') of dielectric permittivity of 0.25% CdSe doped FLC decrases % than the undoped ferroelectric liquid crystal whereas at higher concentration 1% of CdSe quantum dot, loss again increases due to agglomeration or aggregation of CdSe Quantum dot in FLC matrix, which restricts the motion of electrical dipoles in FLC composite.
- Polarization and electro-optic switching response of CdSe doped FLC shows improvement in response time during the application of electric field.

Hence we conclude that synthesized TGA capped CdSe quantum dots improves the ferroelectric switching and dielectric responses of FLC composites.